Groundwater Modeling CVEN4383
Professor: Roseanna Neupauer

IMPLEMENTATION AND SIMULATION OF FLOW AND TRANSPORT MODEL OF YOUNGSTOWN GROUNDWATER AQUIFER TO PROPOSE NEW PUMPING SCHEME

Anders Thufvesson Retzner
University of Colorado

May 3, 2017

Contents

1 Problem Statement

The purpose of this technical document is to present a groundwater pumping scheme to the city of Youngstown, California. The city is expanding its groundwater pumping capacity but fears it has potential to be contaminated by Methyl tert-butyl ether (MTBE), a gasoline additive, which has been observed near a gas station. The proposed pumping scheme should contain information as to which wells should be activated or not activated and at what pumping rate they should be operated such that no drinking water exceeds the primary drinking water standard for MTBE of 0.013mg/L.

To provide a pumping scheme which meets the requirements set by the client, a flow and transport model is setup to simulate groundwater flow in the aquifer. Head observations and MTBE concentration observations and well information is used to create a model representing the site. An aerial view of Youngstown is proved in figure 1.

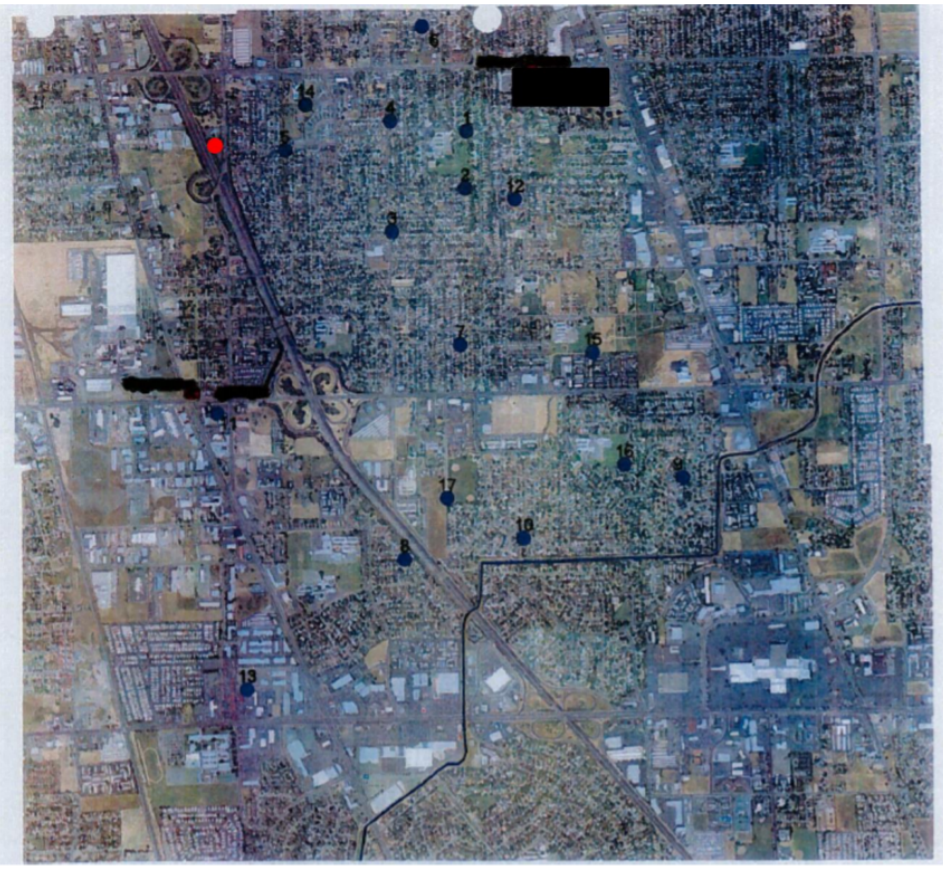

Figure 1: Areal view of the city of Youngstown. Location of the gas station is indicated by a red dot, pumping wells and respective well number is indicated by a blue circle.

2 Conceptual Model

The aquifer is an approximately 50m thick unconfined aquifer which consists of a sandy deposit bounded below by bedrock. Figures 2 and 3 show land surface elevation, bedrock elevation and material type at each pumping well and monitoring well. Since all well logs show one type of material, the aquifer is considered homogeneous. The aquifer is assumed to be isotropic.

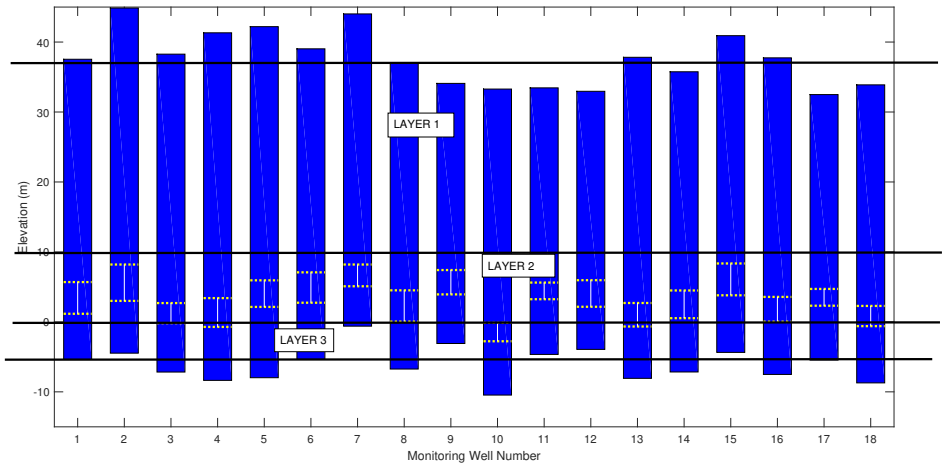

Figure 2: Geometry of monitoring wells. Every blue bar represents one well where the top of the bar is the land surface elevation, the bottom of the bar is the bedrock elevation, the length in between the two white lines represent the screened interval of the well and the color represent the material type.

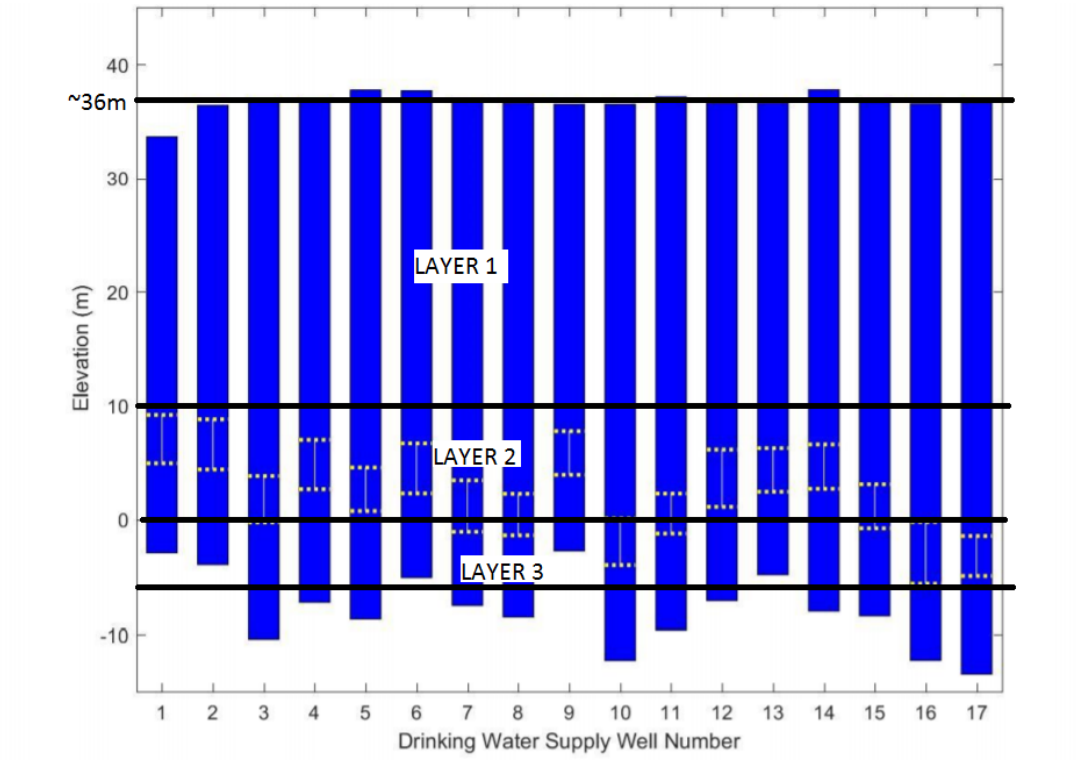

Figure 3: Geometry of pumping wells. Every blue bar represents one well where the top of the bar is the land surface elevation, the bottom of the bar is the bedrock elevation, the length in between the two white lines represent the screened interval of the well and the color represent the material type.

Further information for each pumping and monitoring well is available in section 9.1.1 and 9.1.2.

Prior to pumping, the general direction of groundwater flow is northwest to southeast, see figure 4. To reflect this, the model domain is at a 25° angle. The location of the model is chosen to be centered around the cone of depression that emerges from pumping in 2016, see figure 5. The aquifer is far from any natural hydrological boundaries and no surface water bodies exist in the region. The boundary of the model is therefore considered to be of time-varying specified head type generated from head observations at different times.

The model runs from April 30, 2002, to December 31, 2032. April 30 2002 represents the steady state of the aquifer used to generate initial conditions. From 2002 to 2017 groundwater was used in drinking water supply, affecting the head distribution in the aquifer. The purpose of the model is to analyze and propose a pumping scheme from 2017 to 2032 and so the model runs to December 31 2032.

Natural recharge is known in the region and acts as a source of water. Pumping wells within the model domain act as sinks of water. The only source of MTBE is the leaking

gas station. Pumping wells act as sinks of MTBE.

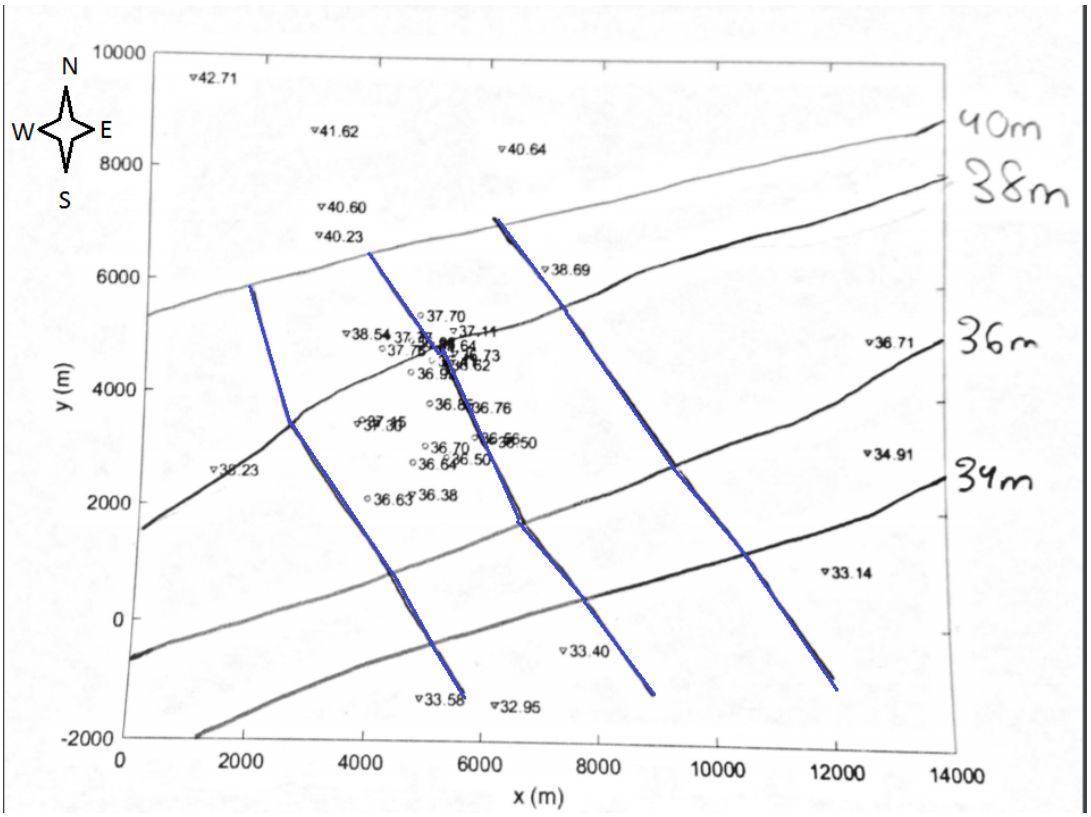

Figure 4: Head contours based on observed heads from 2002. Blue lines show groundwater flow.

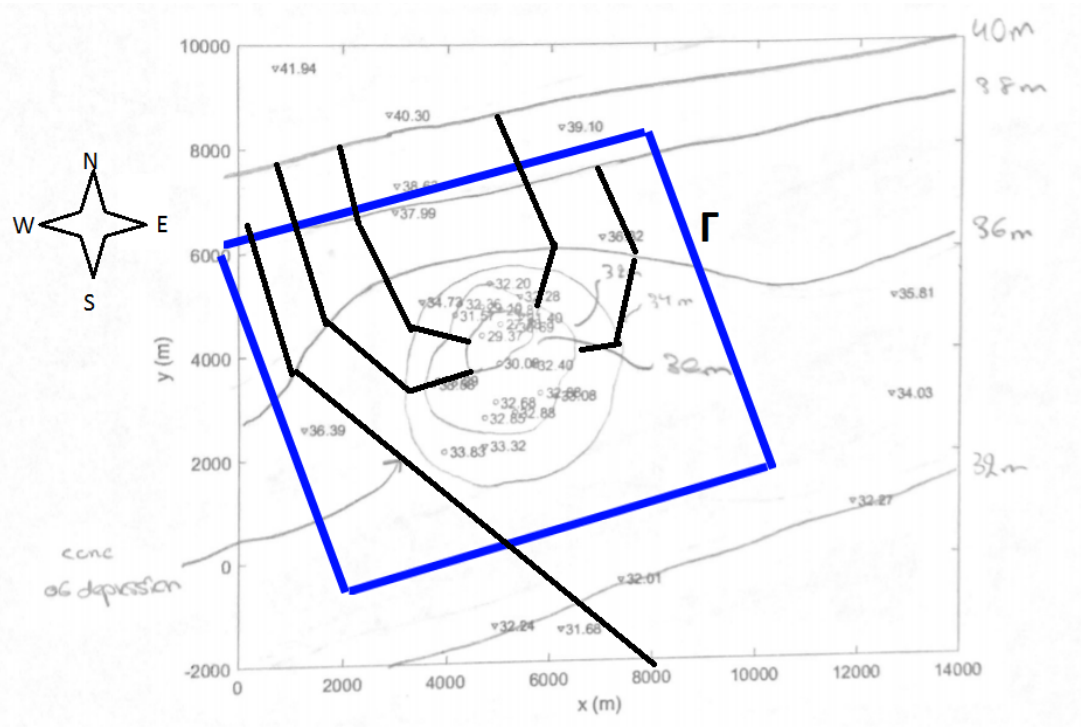

Figure 5: Head contours based on observed heads from 2016. Model is area boxed in by blue borders. Black lines show groundwater flow.

3 Mathematical Model

The aquifer is discretized into three layers with the top layer (layer 1) being unconfined, the layer below (layer 2) and the bottom layer (layer 3) are considered confined.

The top layer is an unconfined aquifer which is governed by

$$\nabla \cdot [K(h_1 - \zeta)\nabla h_1] - \frac{K_z}{b_{12}}(h_1 - h_2) + N = S_y \frac{\partial h}{\partial t} \tag{1}$$

where $h_1 = h_1(\mathbf{x})$ and $h_2 = h_2(\mathbf{x})$ are heads in layer 1 and 2 at spatial coordinate $\mathbf{x} = (x, y)$, K is the horizontal hydraulic conductivity, K_z is the vertical hydraulic conductivity, b_1 is the thickness of layer 1, b_{12} is the thickness of layer 1 and 2, ζ is the elevation of the bottom of the unconfined aquifer, N is natural recharge and S_y is specific yield.

Layer 2 is confined and is governed by

$$\nabla \cdot T\nabla h_2 + \frac{K_z}{b_{12}}(h_1 - h_2) - \frac{K_z}{b_{23}}(h_2 - h_3) - \sum_{i=1}^{N_w} Q'_{i,2}\delta(\mathbf{x} - \mathbf{x}_{w,i}) = S\frac{\partial h}{\partial t} \tag{2}$$

where T is the transmissivity, $h_3 = h_3(\mathbf{x})$ is the head in layer 3 at spatial coordinate $\mathbf{x}$, b_{23} is the thickness of layer 1 and 2, N_w is the number of pumping wells, $Q'_{i,2}$ is the pumping rate of well i per unit aquifer thickness in layer 2 located at spatial coordinate $\mathbf{x}_{w,i}$ and S is the storage coefficient.

Layer 3 is confined and governed by

$$\nabla \cdot T\nabla h_3 + \frac{K_z}{b_{23}}(h_2 - h_3) - \sum_{i=1}^{N_w} Q'_{i,3}\delta(\mathbf{x} - \mathbf{x}_{w,i}) = S\frac{\partial h}{\partial t} \tag{3}$$

where $Q'_{i,3}$ is the pumping rate of well i per unit aquifer thickness in layer 3.

Boundary type is time-varying specified head such that

$$h_1(\mathbf{x}, t) = h_{s,1}(\mathbf{x}, t) \text{ at } \Gamma,$$

$$h_2(\mathbf{x}, t) = h_{s,2}(\mathbf{x}, t) \text{ at } \Gamma,$$

$$h_3(\mathbf{x}, t) = h_{s,3}(\mathbf{x}, t) \text{ at } \Gamma$$

where $h_{s,1}$,$h_{s,2}$ and $h_{s,3}$ are specified heads in layer 1, 2 and 3 respectively at location $\mathbf{x}$ and time t.

Initial conditions are identical for each layer such that

$$h_1(\mathbf{x}) = h_{0,1}(\mathbf{x}) \text{ at } t = 0$$

$$h_2(\mathbf{x}) = h_{0,2}(\mathbf{x}) \text{ at } t = 0$$

$$h_3(\mathbf{x}) = h_{0,3}(\mathbf{x}) \text{ at } t = 0$$

where $h_{0,1}$, $h_{0,2}$ and $h_{0,3}$ is specified initial head at location $\mathbf{x}$ in layer 1, 2 and 3 respectively.

The transport model is given by

$$n\frac{\partial C}{\partial t} = \nabla \cdot n\mathbf{D}\nabla C - \nabla \cdot n\mathbf{v}C - \sum_{i=1}^{N_w} Q'_i C\delta(\mathbf{x} - \mathbf{x_w}) \tag{4}$$

where C is the concentration of MTBE and $\mathbf{D}$ is the dispersion coefficient tensor.

4 Numerical Formulation

4.1 Software and Programming Language

The flow model is represented using MODFLOW-2005 from the United States Geological Service (Harbaugh et al., 2017; Harbaugh, 2005) which is a three-dimensional finite-difference groundwater model. The transport model is simulated using the groundwater solute transport simulator MT3DMS (Tonkin et al., 2016; Bedekar et al., 2016). Both are implemented using the software Processing Modflow (Chiang and Kinzelbach, 2003).

4.2 Spatial Discretization

The horizontal model domain is created at a 25° angle compared to the horizontal grid in the project description, see figure 5. It extends 7000m from its southwest corner to its northwest corner and 9000m from its northwest corner to its northeast corner. The choice is based on the head contours in the region and the cone of depression due to pumping shown in the previous project delivery. The model domain is created such that by it boundaries, head is not affected by the pumping, i.e. far enough away from the cone of depression. By using grid blocks of 50m×50m, the domain is discretized into 140 rows and 180 columns.

The vertical domain is discretized into three layers to capture the varying elevations of the screening of the pumping wells. Top elevation and bottom elevation of each layer is seen in table 1 and can be seen overlain on the geometry of monitoring and pumping wells in figures 2 and 3. The three layer discretization allows for a more accurate predictions of well contamination as for example pumping wells 16 & 17 will only be located in layer 3.

The aquifer is unconfined, however MODFLOW only allows for the top layer to be unconfined since its has the water table as the top of the aquifer. Subsequently, layers 2 & 3 will be treated as 'unconfined/confined' layers with variable transmissivity.

Table 1: Top and bottom elevation for each layer in the model.

Layer	Top Elevation [m]	Bottom Elevation [m]	Layer Type
1	36	10	Unconfined
2	10	0	Unconfined/Confined
3	0	-5	Unconfined/Confined

The wells and their pumping rates are setup in the model. Implementation of the

pumping rates is done by considering the vertical discretization of the model (figure 3), if for example half of the screened interval of a well is located in layer the pumping rate of the well in that layer is half of the well's total pumping rate. The ratios of how much of the screened interval is contained within a layer are approximated by hand and can be seen in table 2.

Table 2: Ratio of screened interval in each layer for every pumping well. Ratios are approximative. No pumping well has any screening in layer 1.

Well Number	Ratio in Layer 2	Ratio in Layer 3
1-6	1	0
7	0.8	0.2
8	0.6	0.4
9	1	0
10	0	1
11	0.7	0.3
12-15	1	0
16	0	1
17	0	1

4.3 Temporal Discretization

Stress periods are added to the model to represent the different time periods in which a certain parameter changes. This is based off pumping schemes and information as to when MTBE has been released and can be seen in table 3. Stress Period 0 is used to generate steady state initial heads for the following stress period. Thus, stress period 0 is run as steady state and all other stress periods as transient.

Table 3: Temporal discretization into stress periods. Stress Period 0 is an arbitrary stress period used to generate steady state initial heads for stress period 2. All stress periods except stress period 0 are transient simulations.

Stress Period	Start Date	End Date	Info
0	-	-	Generate initial heads
1	5/1/02	5/31/10	Start of Pumping
2	6/1/10	6/1/11	Release of MTBE
3	6/2/11	3/31/17	No Release of MTBE
4	6/1/17	12/31/32	New Pumping Rates

Each stress period must be assigned a time length, number of time steps and a

multiplier. Since this model is set up in days as its time unit, one time step is one (1) day. The time length of each stress period is the number of days of the stress period. The number of time steps is determined, for each layer, such that the first time step, Δt_0, satisfies

$$\Delta t_0 < \frac{S_y(\Delta x)^2}{4K\bar{h}}, \tag{5}$$

where $S_y = 9.4 \cdot 10^{-4}$ for layer 1 and replaced by $S_s = 3 \cdot 10^{-3}$ for layer 2 and 3, $\Delta x = 50$m is the spatial (horizontal) discretization, $K = 18$m/d and $\bar{h} \approx 27$m is the most conservative initial saturated thickness. This results in an initial time step of 0.0012 days for layer 1, 0.0039 days for layer 2 and 0.0039 days for layer 3. The most restrictive time step allowed of 0.0012 days is used.

The number of time steps, n_{steps}, is determined for each stress period as

$$n_{steps} = \frac{\log[t_0 + L(r-1)] - \log(t_0)}{\log(r)} \tag{6}$$

where $t_0 = 0.0012$ days is the length of the initial time step, L is the length of the stress period and r is the multiplier. All parameters for each stress period are seen in table 4.

Table 4: Length, number of time steps and multiplier for each stress period. Number of time steps were set to nearest highest integer.

Stress Period	Length (L) [d]	Number of Time Steps (n)	Multiplier (r)
0	1	1	1.4
1	2953	41	1.4
2	366	35	1.4
3	2191	41	1.4
4	5693	43	1.4

4.4 Boundary Conditions

The first stress period uses boundary conditions interpolated spatially from observed heads in 2002. Figure 6 shows the interpolated values used as boundary conditions in layer 1, which are also used for layers 2 and 3.

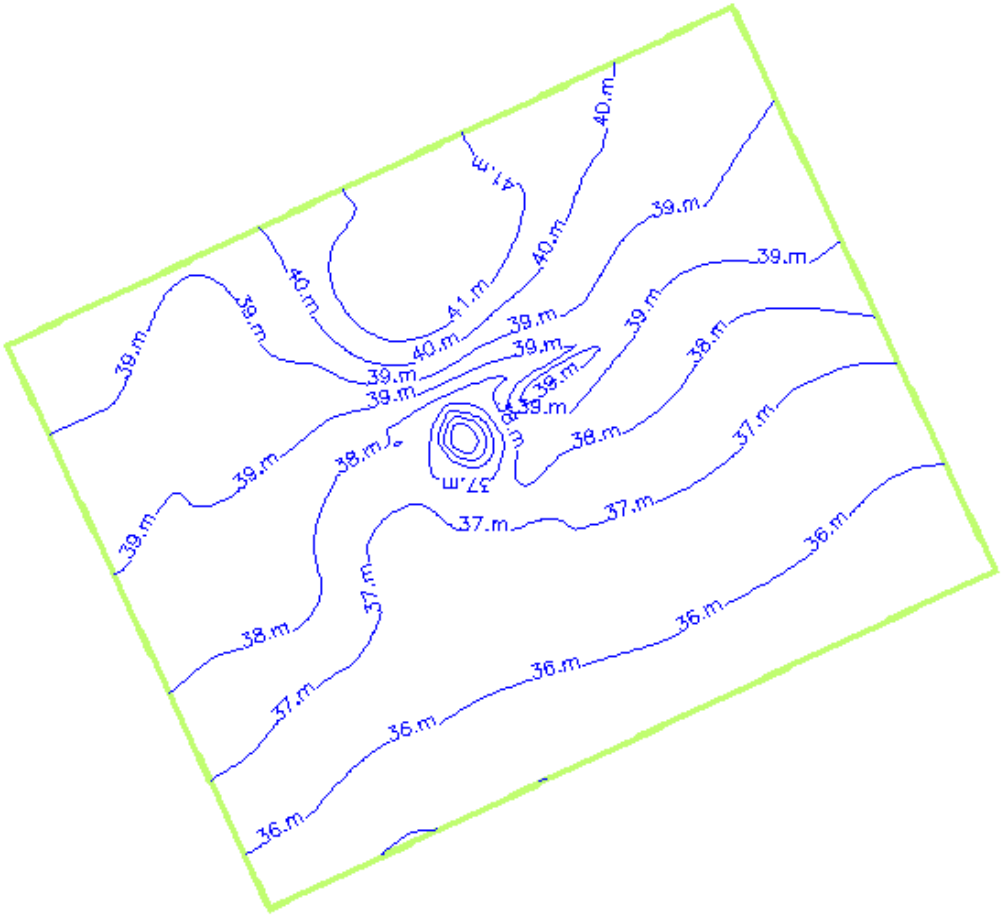

Figure 6: Interpolated heads from observations in 2002 used for steady state boundary conditions.

The transient simulation consists of 4 stress periods. The boundary conditions for each transient stress period are implemented as time-varying specified head boundaries, each with an initial specified head and an 'end' (of stress period) specified head. Observed heads from 2002 and 2012 are available. The observed heads from 2002 are interpolated and used as boundary conditions for the steady state stress periods as both initial and end conditions. The same interpolated heads are then used as initial boundary conditions for stress period 1 (first transient simulation).

To determine the boundary conditions at the end of stress period 1, observed heads are interpolated in time from the observed heads in 2002 and 2012. Head is assumed to be linear in time. The 4 transient stress periods are a total of 11,204 days. The observed heads from 2002 are considered heads at $t = 0$ days and heads from 2012 are considered

heads at $t = 3,650$ days (10 years). Heads are interpolated linearly in time such that

$$h_{s,1}(\mathbf{x}, t) = h_{s,2}(\mathbf{x}, t) = h_{s,3}(\mathbf{x}, t) = h_{02}(\mathbf{x}) + \frac{h_{12}(\mathbf{x}) - h_{02}(\mathbf{x})}{3,650\text{days}} t \text{ at } \Gamma, \tag{7}$$

where h_{02} is observed head from 2002 and h_{12} is observed head from 2012. For example, the boundary heads at the end of stress period 1 is calculated using the previously mentioned equation with $t = 2953$ days. Boundary heads at end of stress period 2 are calculated using $t = 2953$ days $+ 366$ days and so on. Each stress periods initial boundary heads are the same as the previous period's end boundary heads. Figures 7-10 show boundary heads at the end of each stress period. Since the boundary heads are identical for all three layers, only boundary heads in layer 1 are shown.

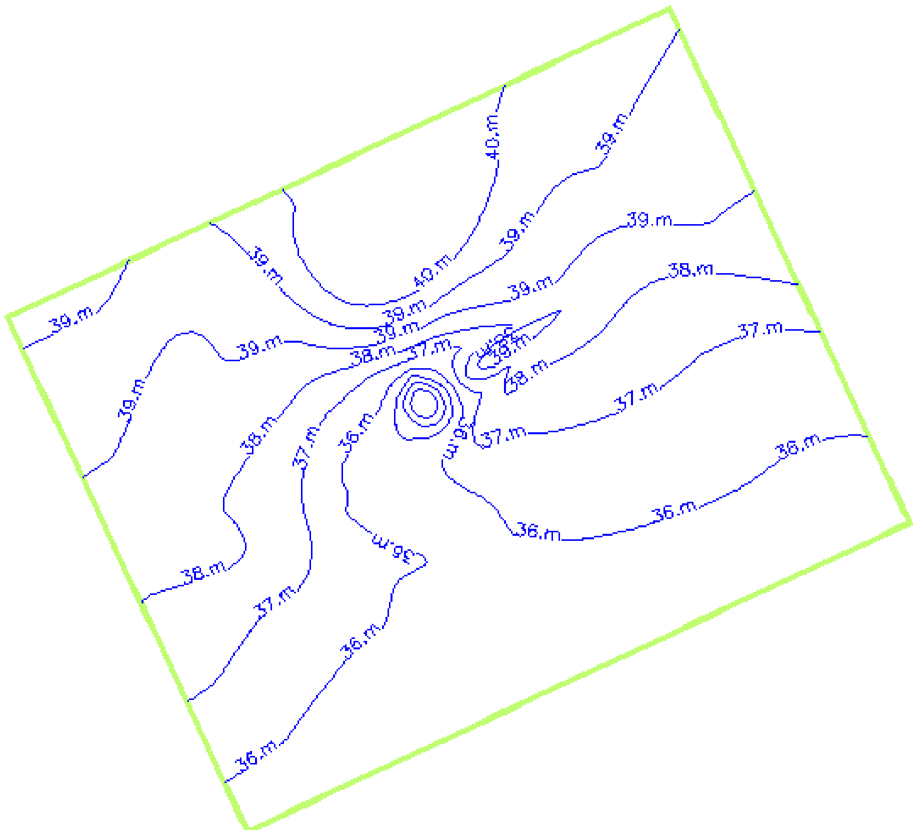

Figure 7: Head contours in layer 1 at the end of stress period 1 from interpolated data used for boundary heads.

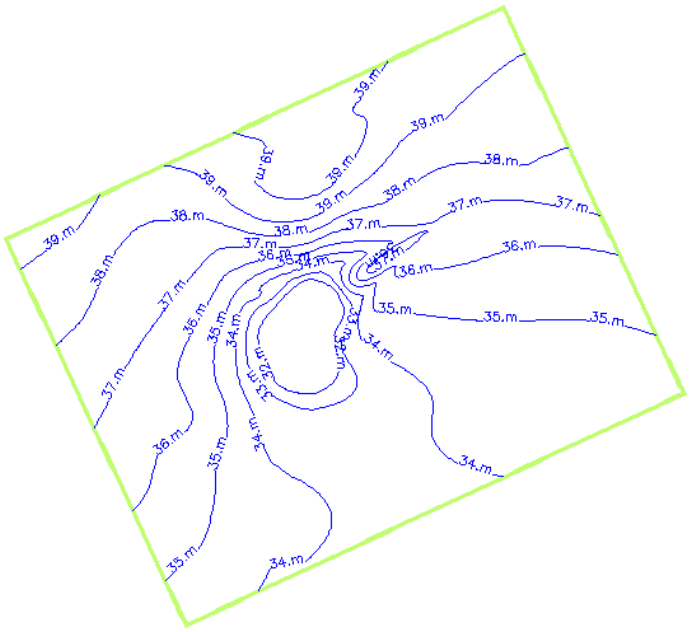

Figure 8: Head contours in layer 1 at the end of stress period 2 from interpolated data used for boundary heads.

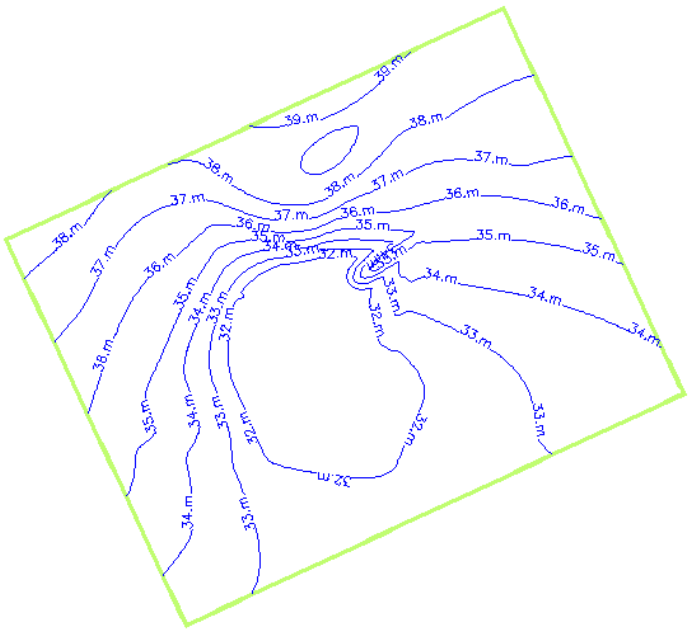

Figure 9: Head contours in layer 1 at the end of stress period 3 from interpolated data used for boundary heads.

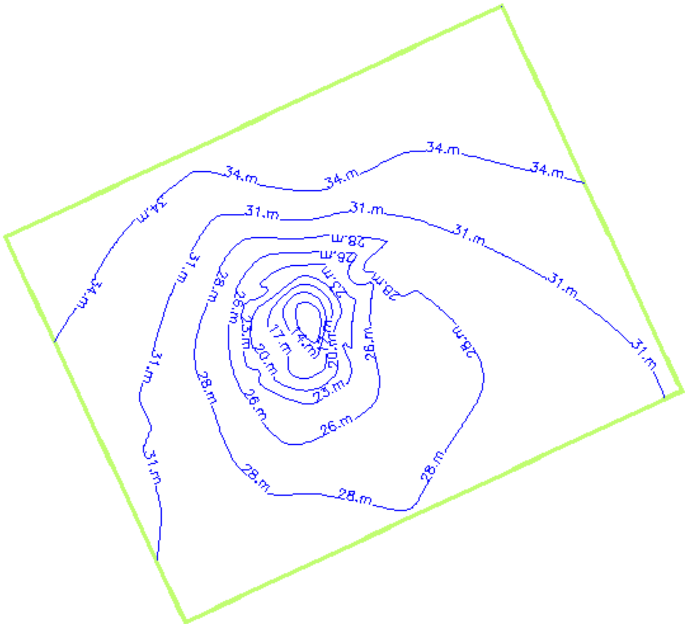

Figure 10: Head contours in layer 1 at the end of stress period 4 from interpolated data used for boundary heads.

4.5 Parameter Values

All parameter values used in the numerical model are shown in table 5.

Table 5: Parameter values as implemented in the numerical model.

Description	Parameter	Value
Horizontal hydraulic conductivity	K	18m/d
Vertical hydraulic conductivity	K_z	0.62m/d
Porosity	n	0.12
Specific Yield	S_y	$9 \cdot 10^{-4}$
Specific Storage	S_s	$3 \cdot 10^{-3}$m^{-1}
Longitudinal dispersivity	α_L	5m
Horizontal transverse dispersivity	α_{TH}	1m
Vertical transverse dispersivity	α_{TV}	0.25m
Natural Recharge	N	$3.559 \cdot 10^{-5}$m/d
Thickness of layer 1	b_1	26m
Thickness of layer 2	b_2	10m
Thickness of layer 3	b_3	5m

All well locations and pumping rates, $\mathbf{x}_{w,i}$ and Q'_i for $i = 1, 2, ..N_w$, are presented in section 9.1.1. Total number of pumping wells, N_w, is 17.

The horizontal hydraulic conductivity is reasonable considering it can vary from less than 1m/d to over 100/md for sand deposits (Anderson, Woessner, and Hunt, 2015; Fitts, 2013, figure 5.25 in Anderson, table 3.2 in Fitts). The ratio of the horizontal and vertical hydraulic conductivity can vary from 10-100 (Fitts, 2013, p. 60) which suggests the vertical hydraulic conductivity used in the numerical model is not unreasonable. A porosity of 12% is below typical values according to Fitts (2013, table 2.2) but not unreasonable. The porosity was set to a low value to match the concentration data provided. Specific yield, set by the calibration, is very small (Fitts, 2013). Specific storage is reasonable considering typical values for the storage coefficient $S = S_s b$ range from 10^{-2} to 10^{-5} (Fitts, 2013, p. 220), where b is the aquifer thickness (36m in this model). The longitudinal dispersivity is small when considering figure 2 in Gelhar, Welty, and Rehfeldt (1992), relating the scale of the transport model to the longitudinal dispersivity. Both transverse dispersivities are reasonable considering they are fractions of the longitudinal dispersivity (Fitts, 2013, p. 548). Natural recharge is approximated for the project site. Thickness of each layer is based upon the geometry of the pumping and monitoring wells seen in figures 3 and 2.

4.6 Initial Conditions for Flow Model

Stress period 0, which is steady state, is used to generate initial conditions for the transient simulation and are shown in figure 11. Initial conditions are identical in all three layers.

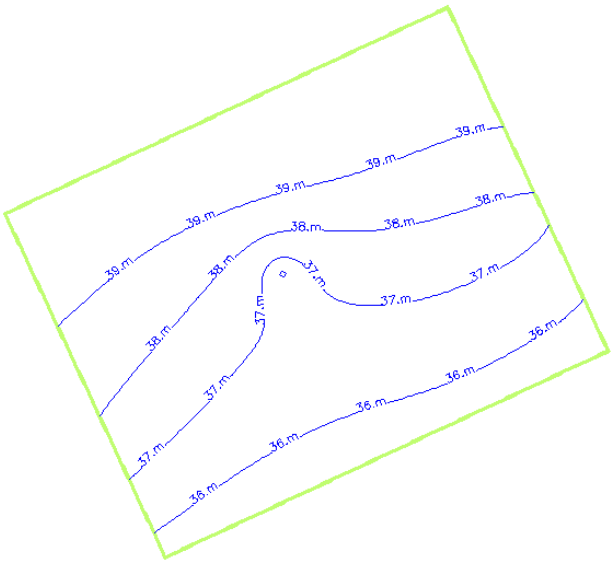

Figure 11: Initial conditions as used in all three layers.

4.7 Initial Conditions for Transport Model

The initial concentration throughout the aquifer is set to 0 as no MTBE is observed at $t = 0$.

4.8 Peclet Number

The Peclet Number, Pe, is determined using the definition in equation 8,

$$Pe = \frac{\Delta x}{\alpha_L} = 10, \tag{8}$$

where $\Delta x = 50$m is the horizontal spatial discretization and $\alpha_L = 5$m is the longitudinal dispersivity.

A general rule is that the Peclet Number should be smaller than 1, which is not the case for this model. To achieve a Peclet Number less than 1, the spatial discretization Δx would have to be smaller than 5m. A model with $\Delta x = 5$m would have taken too long to simulate as this project does not have access to high performance computing.

5 Calibration

5.1 Flow Model Calibration

5.1.1 Calibration Parameters

Horizontal and vertical hydraulic conductivity, K and K_z, specific yield, S_y, and specific storage , S_s, are calibrated. All calibrated parameters are assumed to be constant in time and throughout the aquifer.

5.1.2 Calibration and Verification Data

Calibration and verification data consist of observed heads from pumping wells and monitoring wells, see section 9.2.1. Only wells within the model boundary are used. The data is split into calibration data and verification data, the verification data is set apart by assigning a weight of 0.00001. Calibration data consists of observations from

- monitoring wells 4, 5, 14, 18
- and pumping wells 1, 3, 6, 7, 8, 9, 11, 12, 14, 15.

The verification data thus consists of observations from

- monitoring wells 3, 6, 13, 15, 16,
- and pumping wells 2, 4, 5, 10, 13, 16.

5.1.3 Calibration Targets

Calibration targets are as follows:

$$\sum_{i=1}^{n} \epsilon_i^2 < 15\text{m}^2, \tag{9}$$

$$\max |\epsilon_i| < 0.6\text{m}, \tag{10}$$

$$|\frac{1}{n}\sum_{i=1}^{n} \epsilon_i| < 0.06\text{m}, \tag{11}$$

where $\epsilon_i(\mathbf{x}, t)$ is the ith residual calculated using observed head, $h_i(\mathbf{x}, t)$, and corresponding modelled head, $h_i^*(\mathbf{x}, t)$ such that

$$\epsilon_i(\mathbf{x}, t) = h_i(\mathbf{x}, t) - h_i^*(\mathbf{x}, t).$$

Target 10 is set considering $1/10^{\text{th}}$ of the head drop across the aquifer which is about 6m at $t = 0$.

5.1.4 Calibration Procedure

Calibration of the flow model is handled by a MODFLOW-module called *PEST* (parameter estimation). Each parameter is assigned a minimum, maximum and initial value which are based upon what is thought to be reasonable for the aquifer. The calibration module runs the model a number of times with initial values for each parameter and some variations of these values. The module compares modelled heads to observed heads from the calibration data to determine if it needs to go through another iteration. If so, it changes the parameter values based on a sensitivity analysis. Horizontal hydraulic conductivity and vertical hydraulic conductivity are calibrated using only stress period 0 (steady state). The estimated values are then set to initial guesses when calibrating specific storage and specific storage. Calibration for the storage properties is done using all stress periods and is thus transient. A final calibration, which estimated values are considered 'final', is done using all stress periods and setting the initial guesses of each parameter to the estimated value obtained in previous calibrations.

5.1.5 Final Parameter Values

Final parameter values and confidence limits for each calibrated parameter are shown in table 6.

Table 6: Final parameter values after calibration of flow model. Confidence limits show 95% confidence interval.

Parameter	Estimated Value	Lower Confidence Limit	Upper Confidence Limit
K	18 m/d	17.6 m/d	18.4 m/d
K_z	0.62 m/d	0.49 m/d	0.79 m/d
S_y	$9 \cdot 10^{-4}$	$3 \cdot 10^{-14}$	$3 \cdot 10^{7}$
S_s	$3.0 \cdot 10^{-3}\text{m}^{-1}$	$2.4 \cdot 10^{-3}\text{m}^{-1}$	$3.6 \cdot 10^{-3}\text{m}^{-1}$

5.1.6 Calibration Results

All residuals are found in section 9.2.3. Results of calibration target are:

$$\sum_{i=1}^{n} \epsilon_i^2 = 21\text{m}^2 \quad \text{not OK},$$

$$\max |\epsilon| = 1.2\text{m} \quad \text{not OK},$$

$$|\frac{1}{n}\sum_{i=1}^{n}\epsilon_i| = 0.13\text{m} \quad \text{not OK}.$$

Verification data is also used to evaluate calibration results:

$$\sum_{i=1}^{n}\epsilon_i^2 = 19\text{m}^2 \quad \text{not OK},$$

$$|\epsilon| = 1.3\text{m} \quad \text{not OK},$$

$$|\frac{1}{n}\sum_{i=1}^{n}\epsilon_i| = 0.14\text{m} \quad \text{not OK}.$$

Figures 12-35 show simulated and observed head as a function of time at each well.

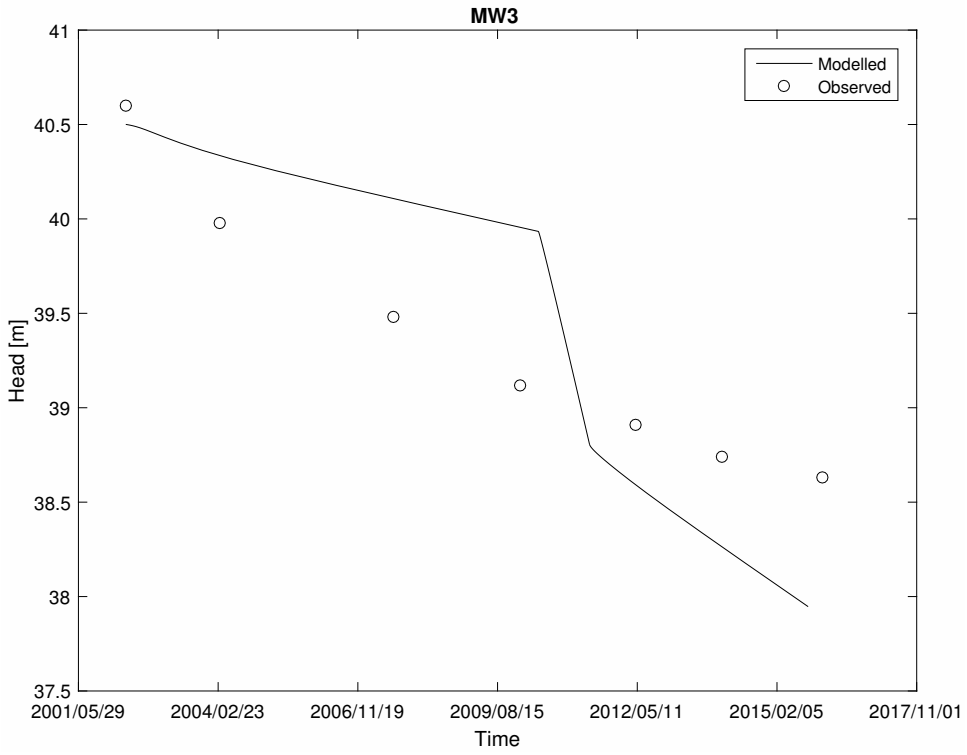

Figure 12: Modelled and observed head at monitoring well 3.

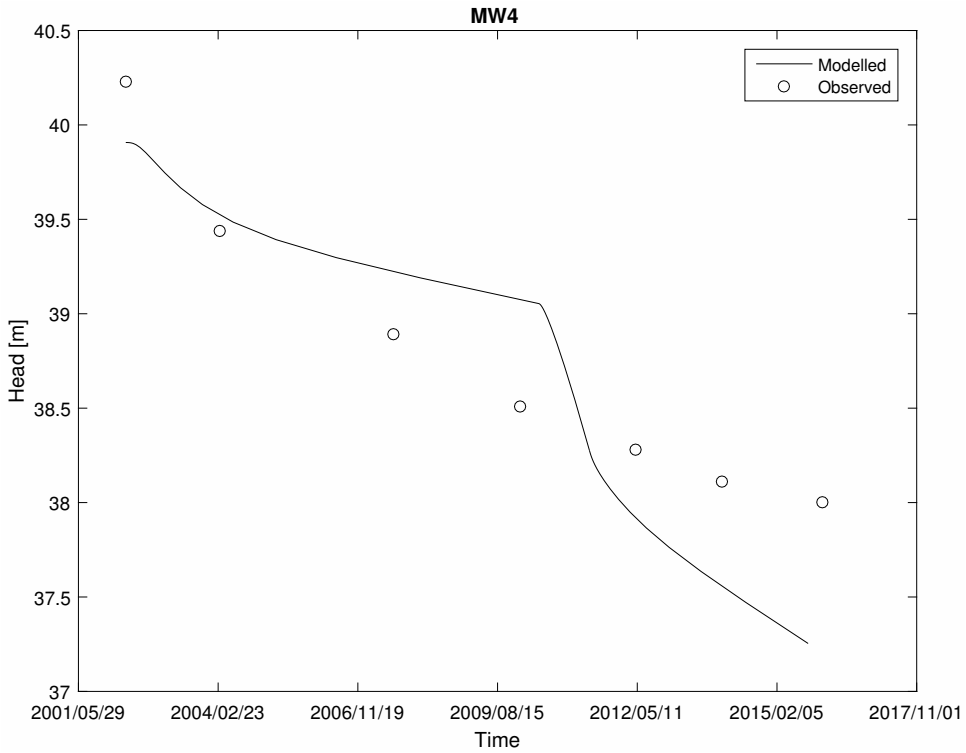

Figure 13: Modelled and observed head at monitoring well 4.

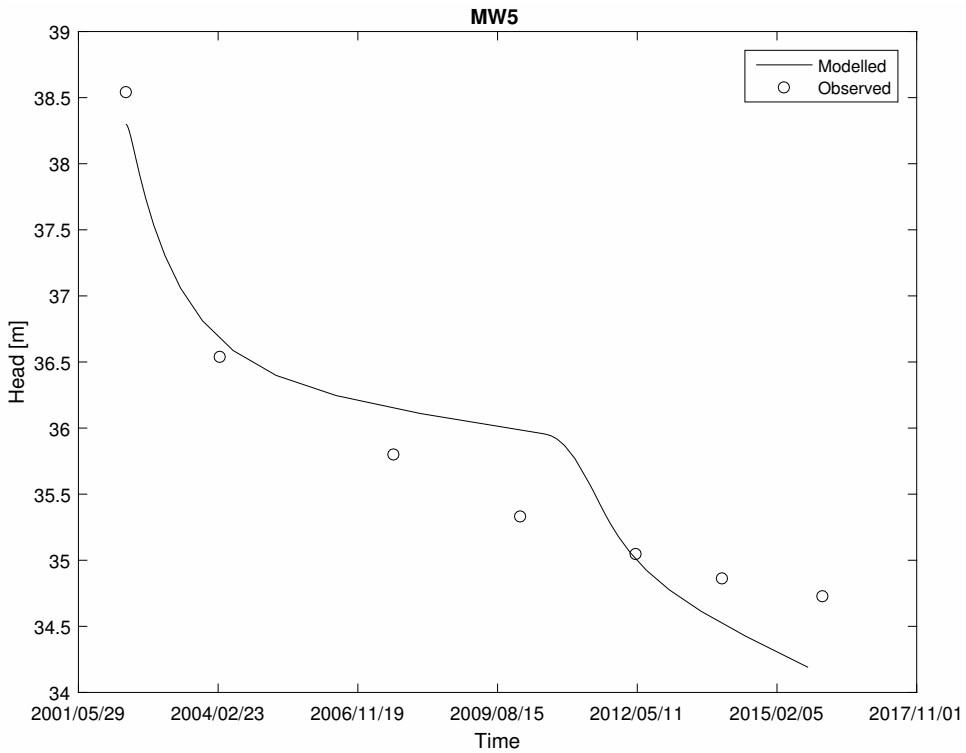

Figure 14: Modelled and observed head at monitoring well 5.

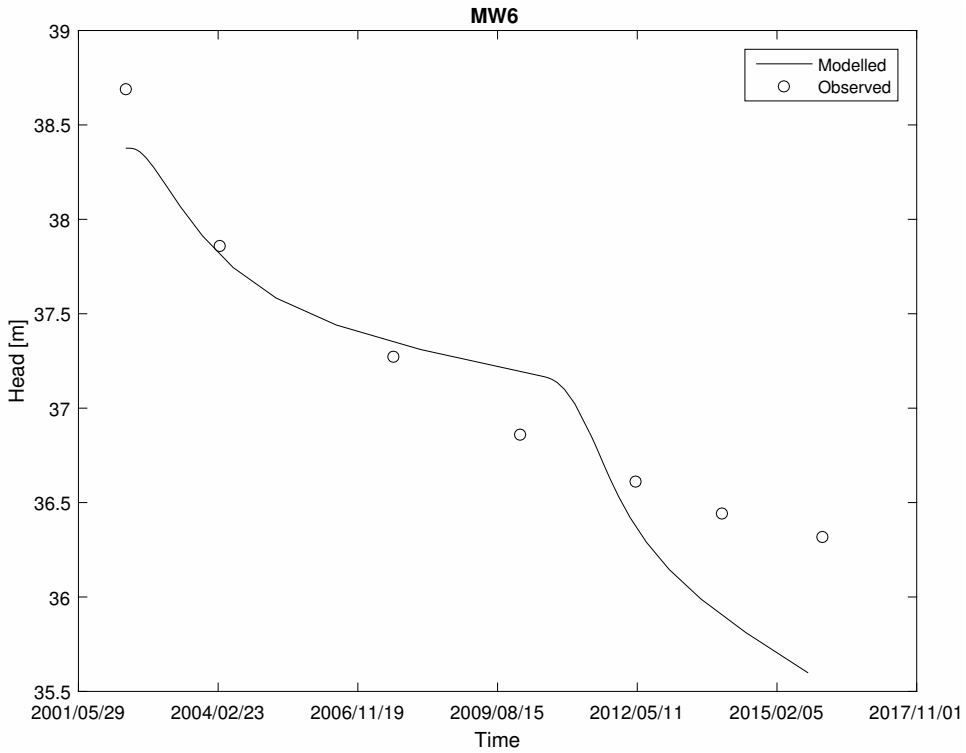

Figure 15: Modelled and observed head at monitoring well 6.

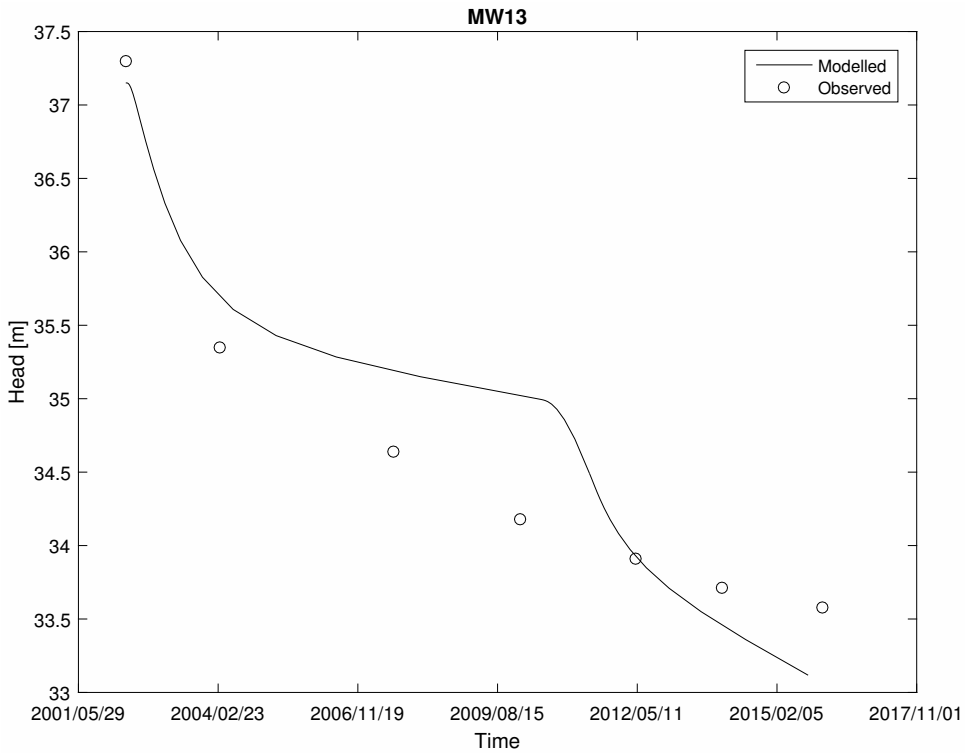

Figure 16: Modelled and observed head at monitoring well 13.

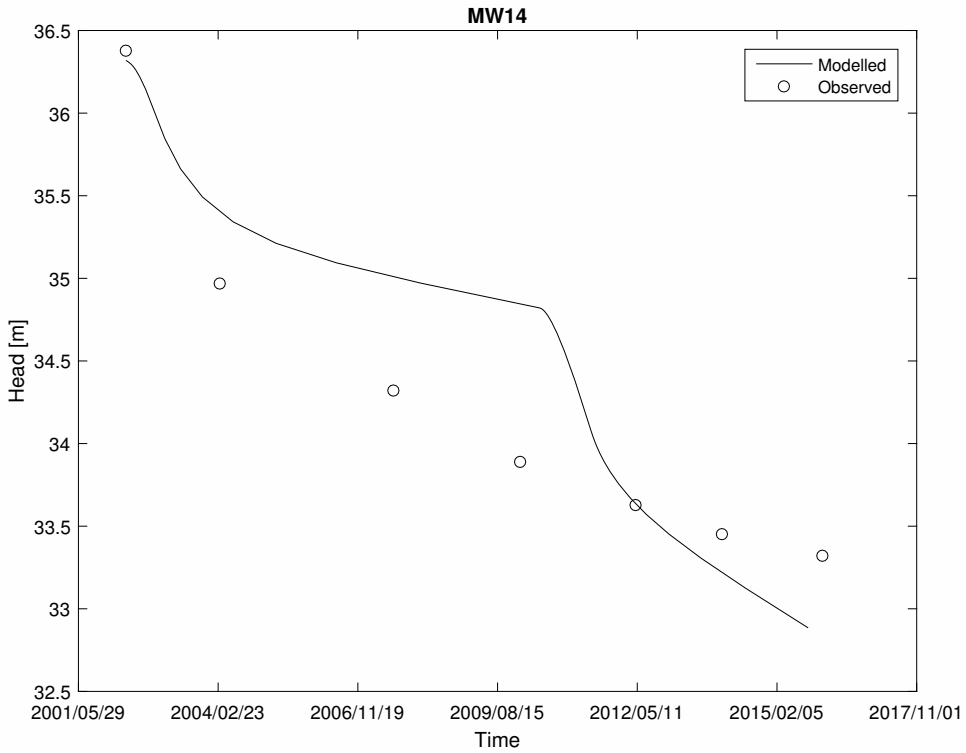

Figure 17: Modelled and observed head at monitoring well 14.

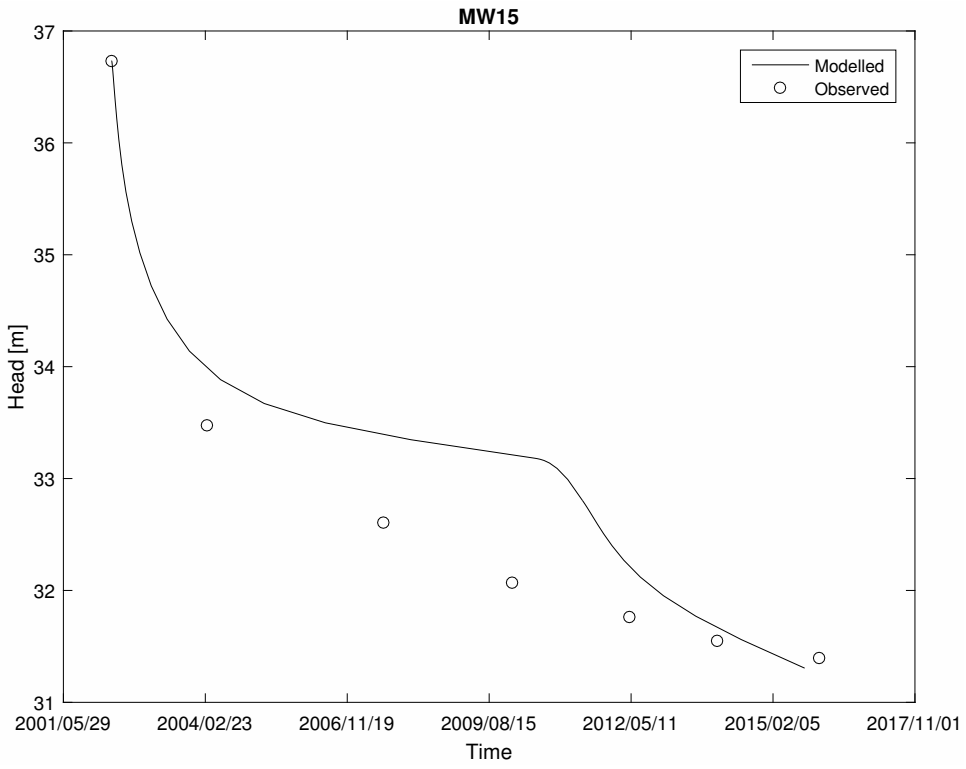

Figure 18: Modelled and observed head at monitoring well 15.

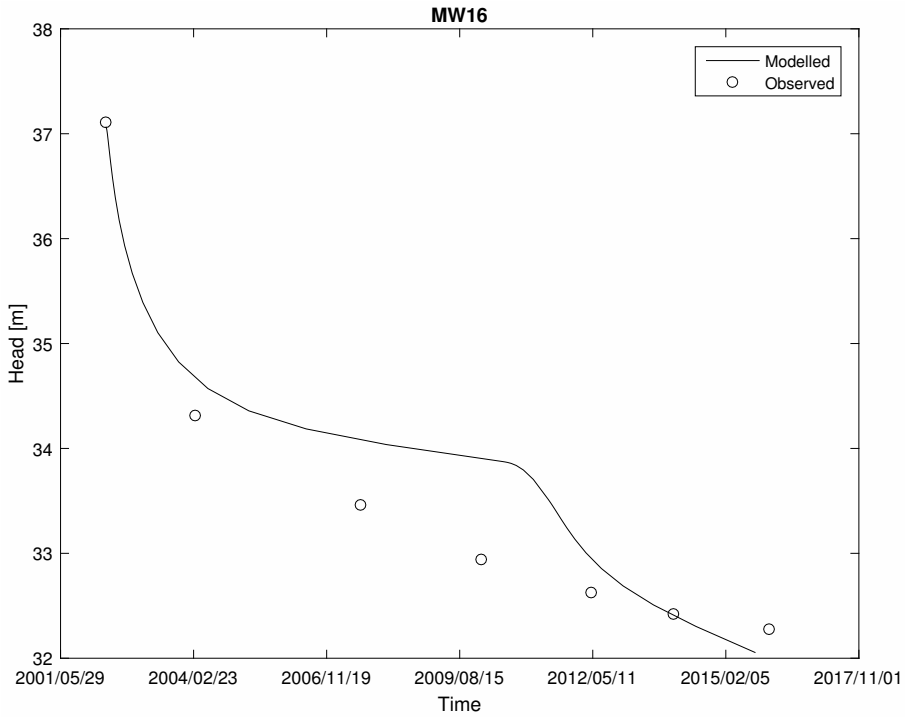

Figure 19: Modelled and observed head at monitoring well 16.

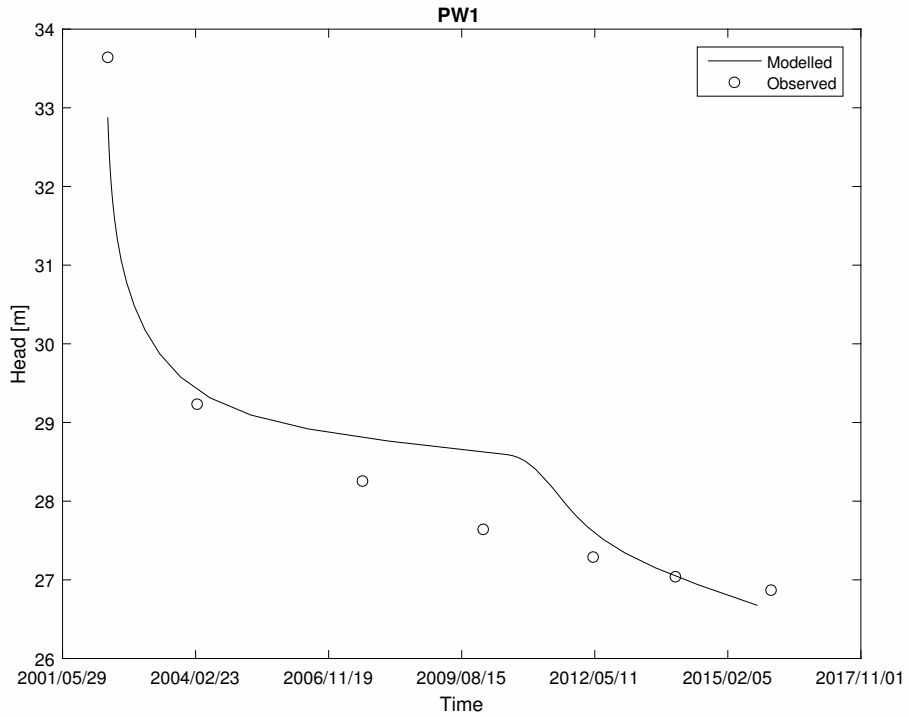

Figure 20: Modelled and observed head at pumping well 1.

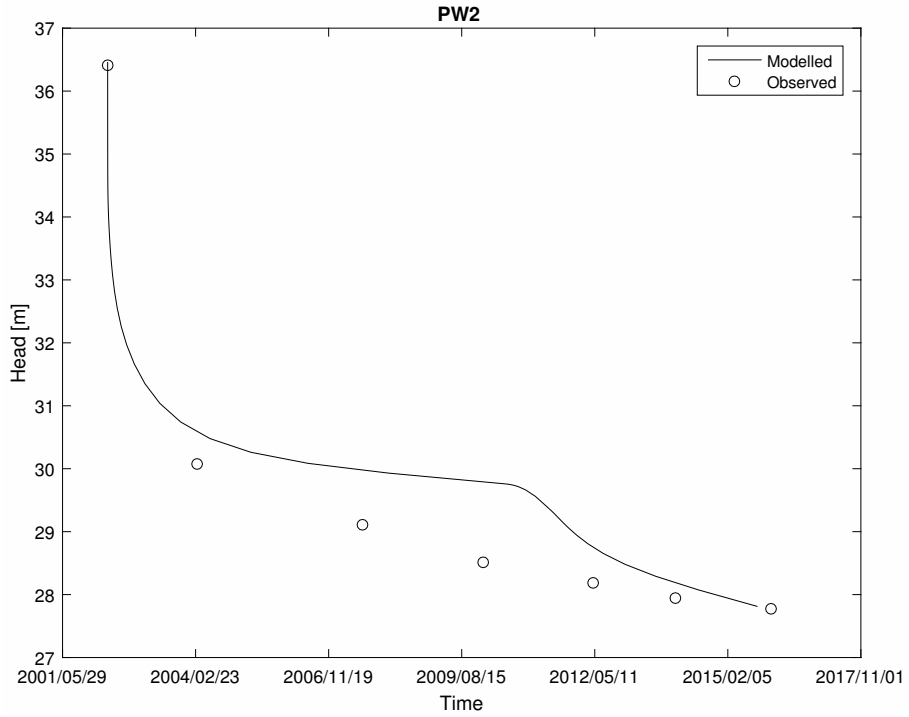

Figure 21: Modelled and observed head at pumping well 2.

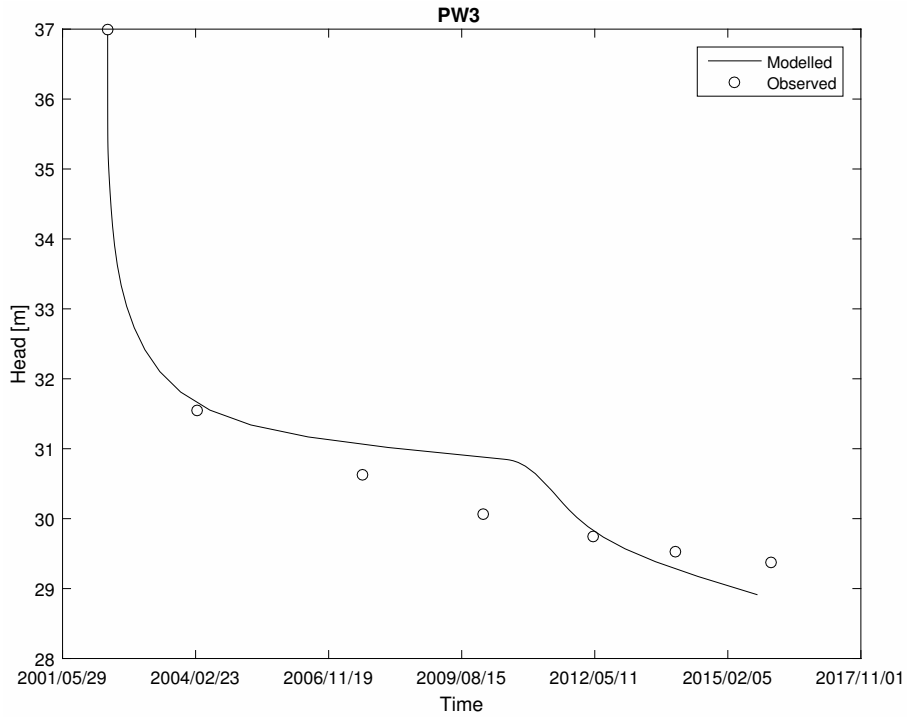

Figure 22: Modelled and observed head at pumping well 3.

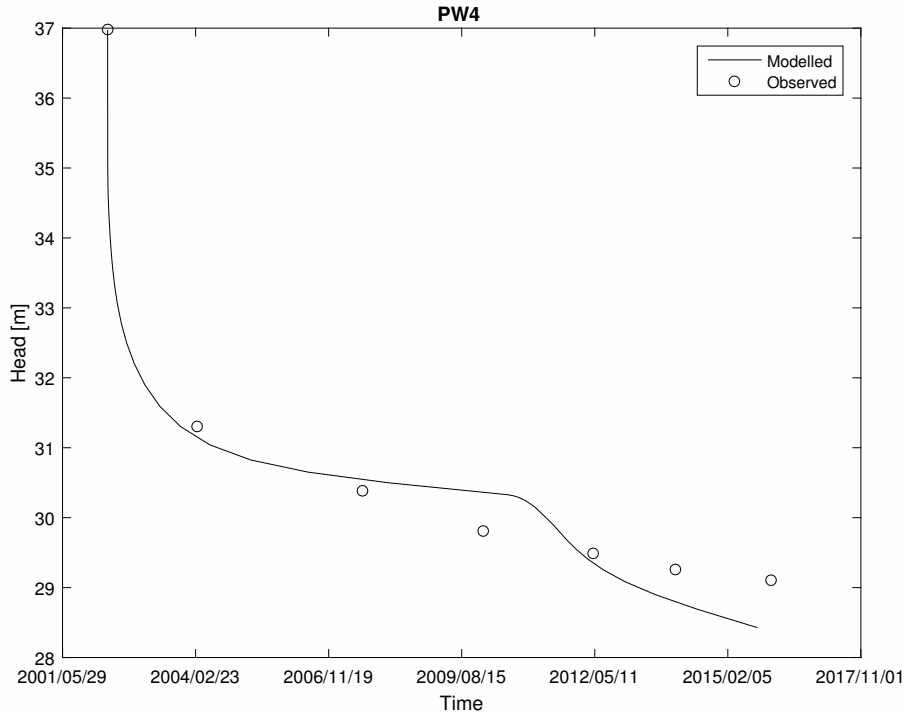

Figure 23: Modelled and observed head at pumping well 4.

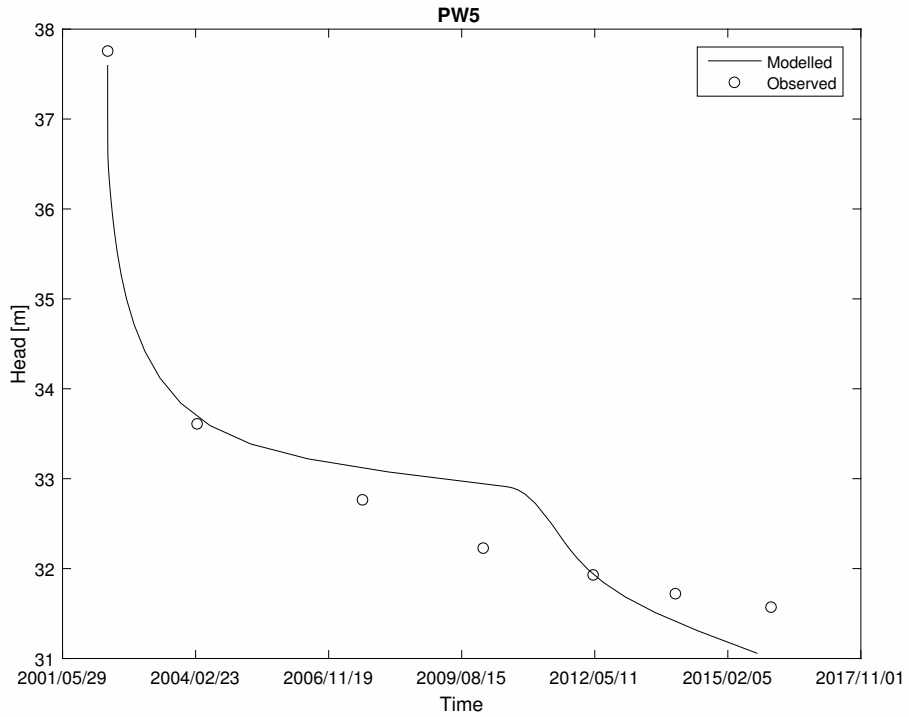

Figure 24: Modelled and observed head at pumping well 5.

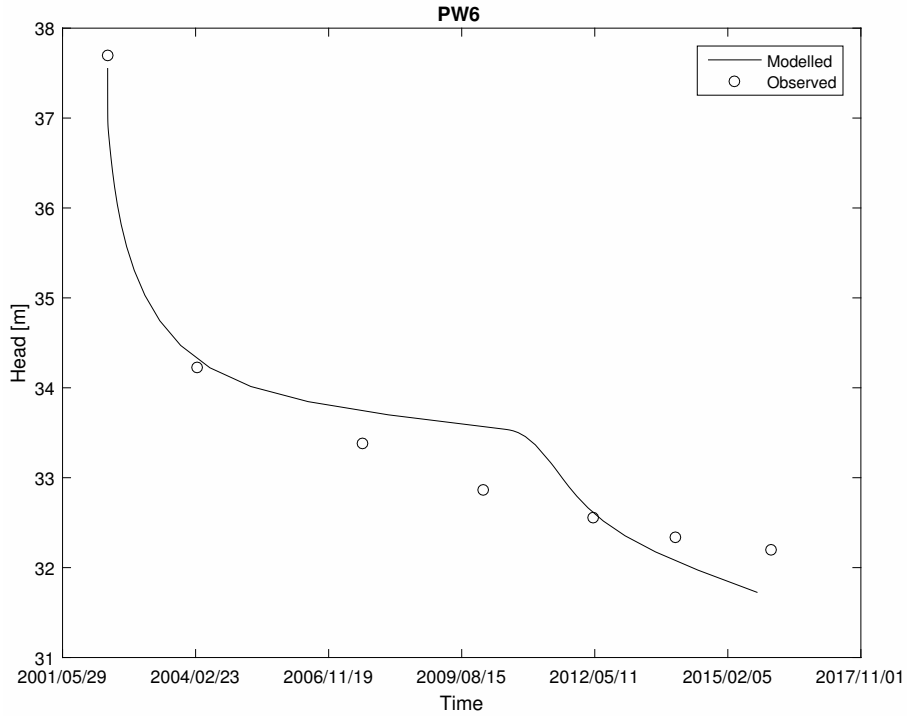

Figure 25: Modelled and observed head at pumping well 6.

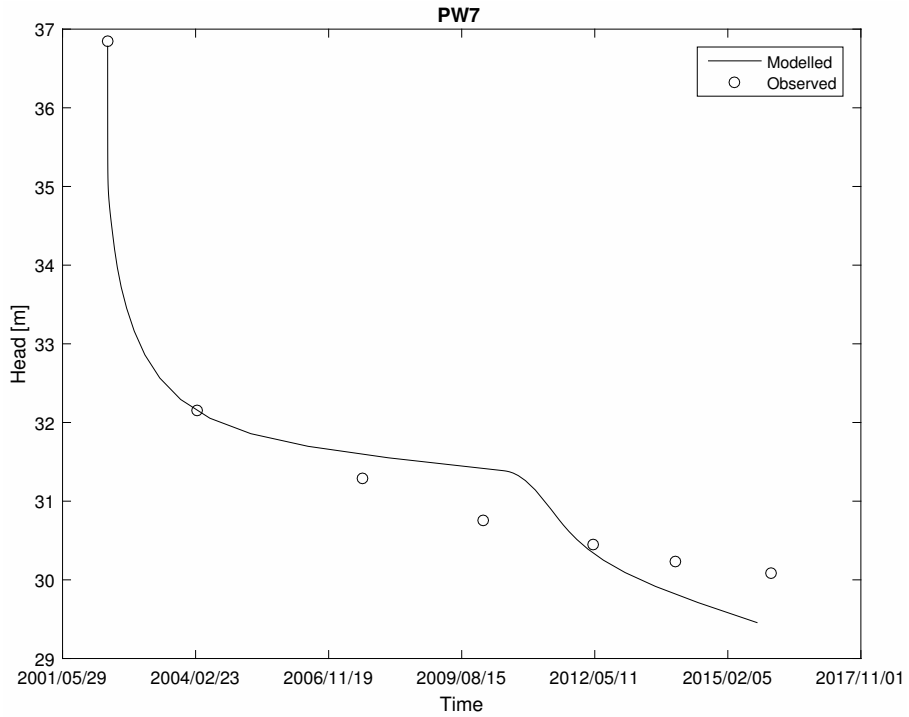

Figure 26: Modelled and observed head at pumping well 7.

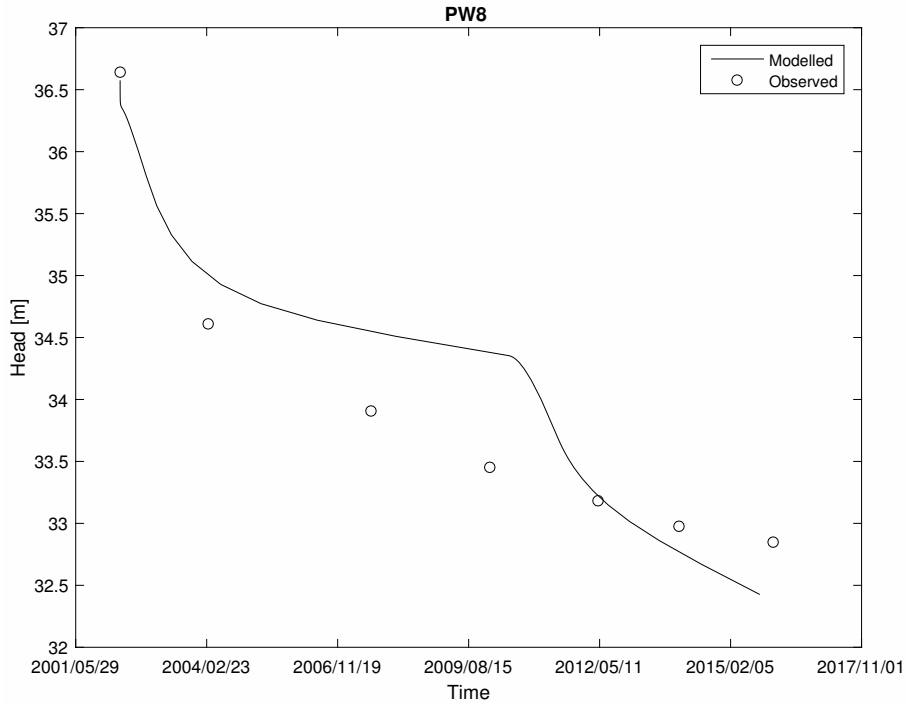

Figure 27: Modelled and observed head at pumping well 8.

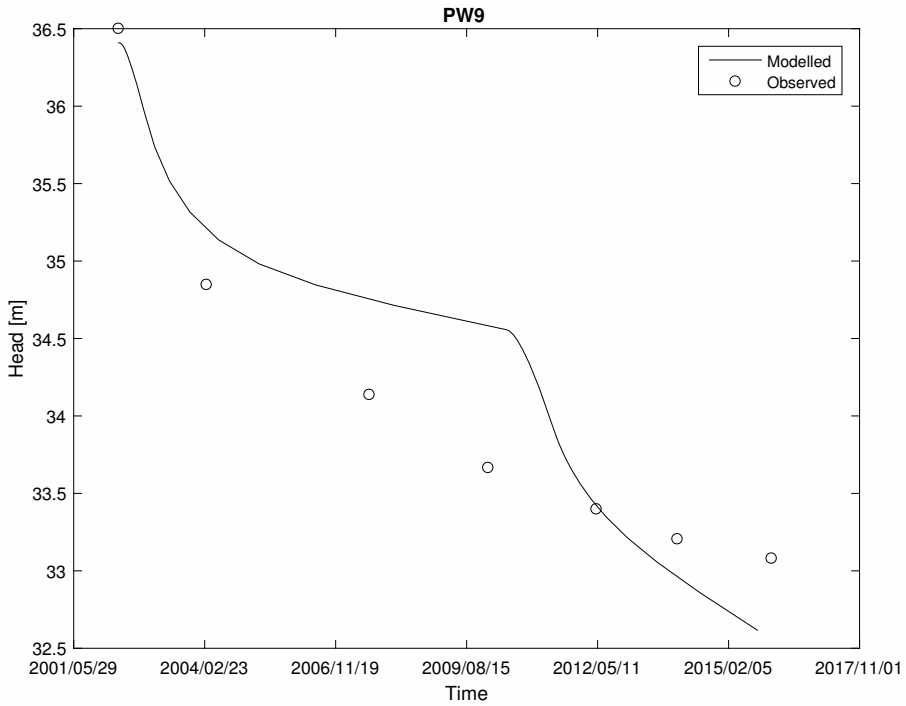

Figure 28: Modelled and observed head at pumping well 9.

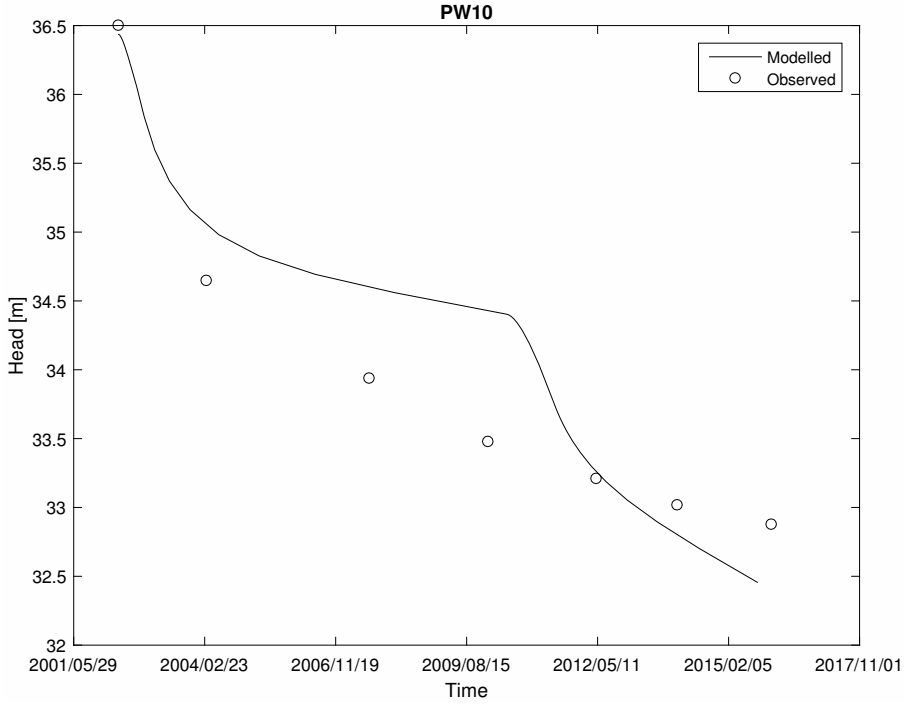

Figure 29: Modelled and observed head at pumping well 10.

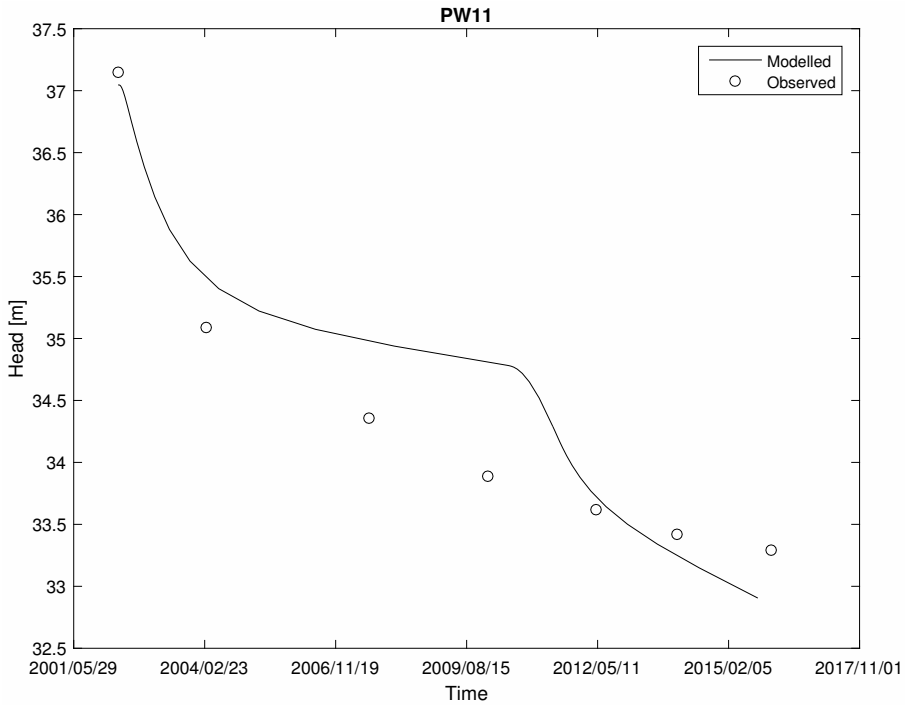

Figure 30: Modelled and observed head at pumping well 11.

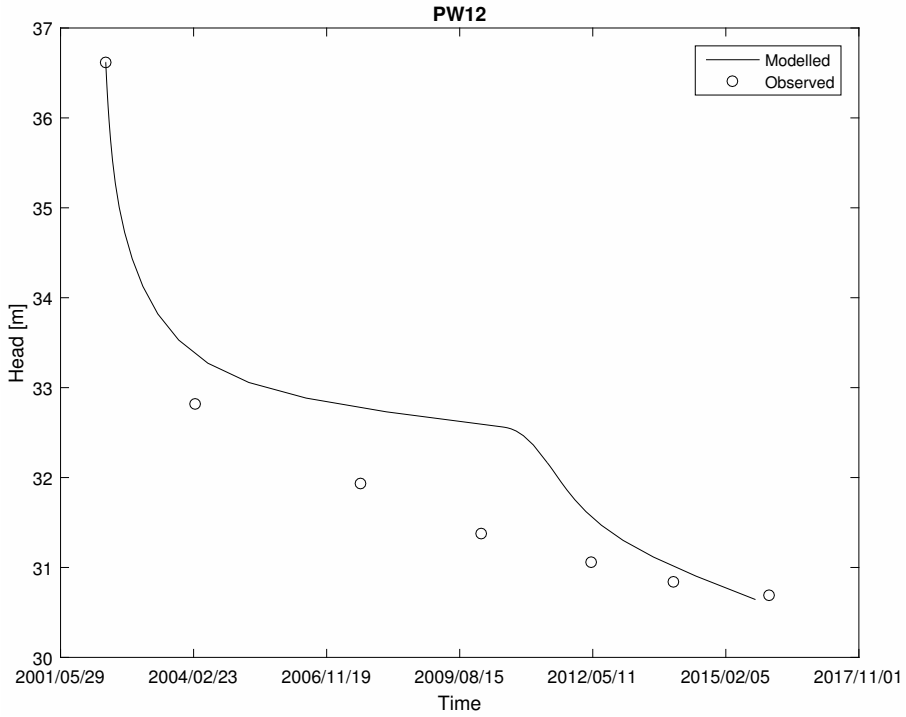

Figure 31: Modelled and observed head at pumping well 12.

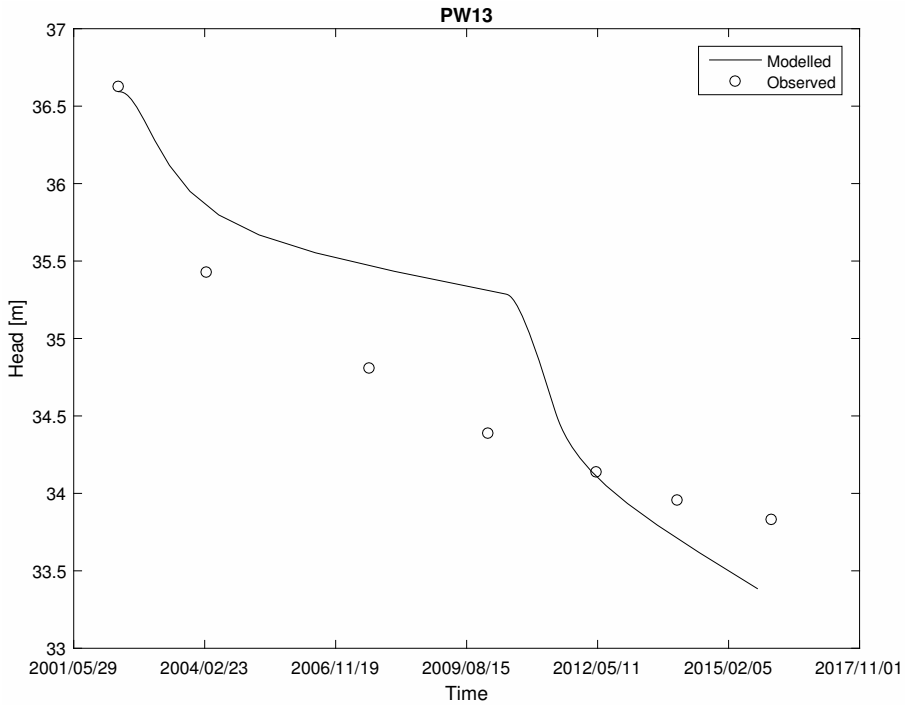

Figure 32: Modelled and observed head at pumping well 13.

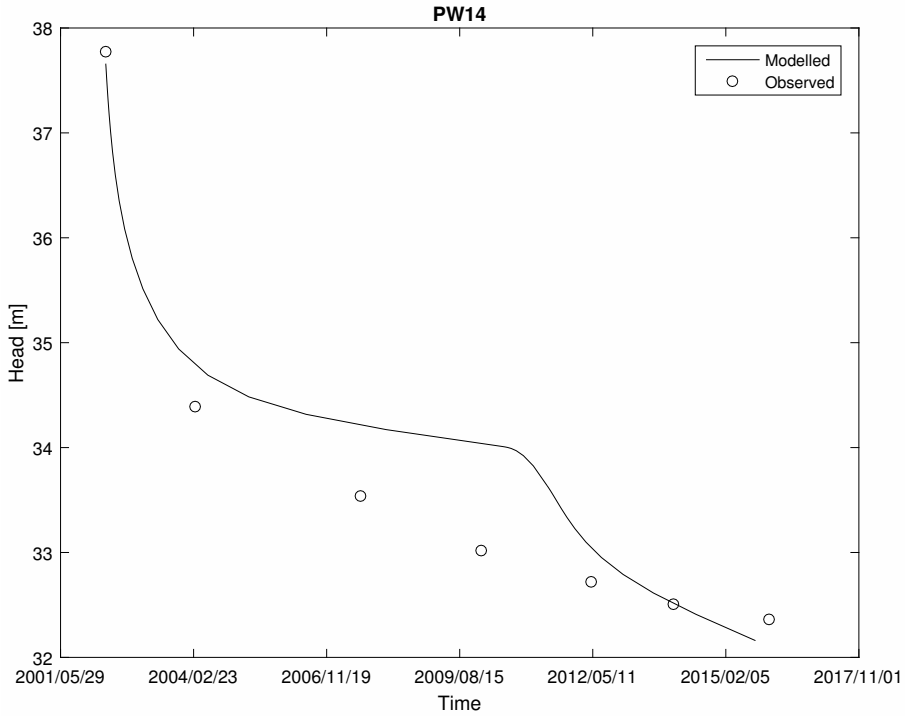

Figure 33: Modelled and observed head at pumping well 14.

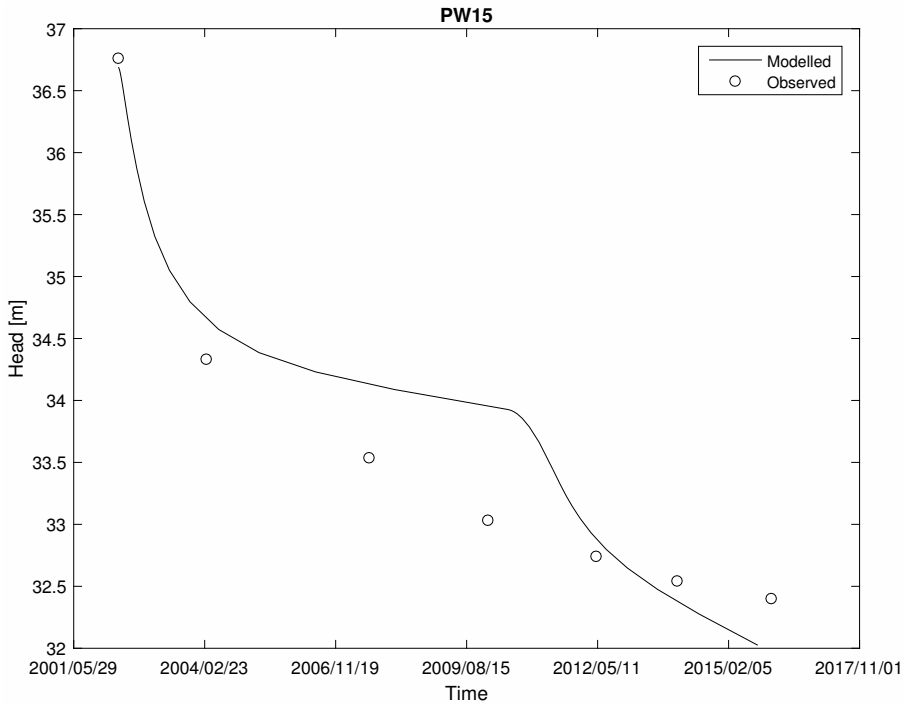

Figure 34: Modelled and observed head at pumping well 15.

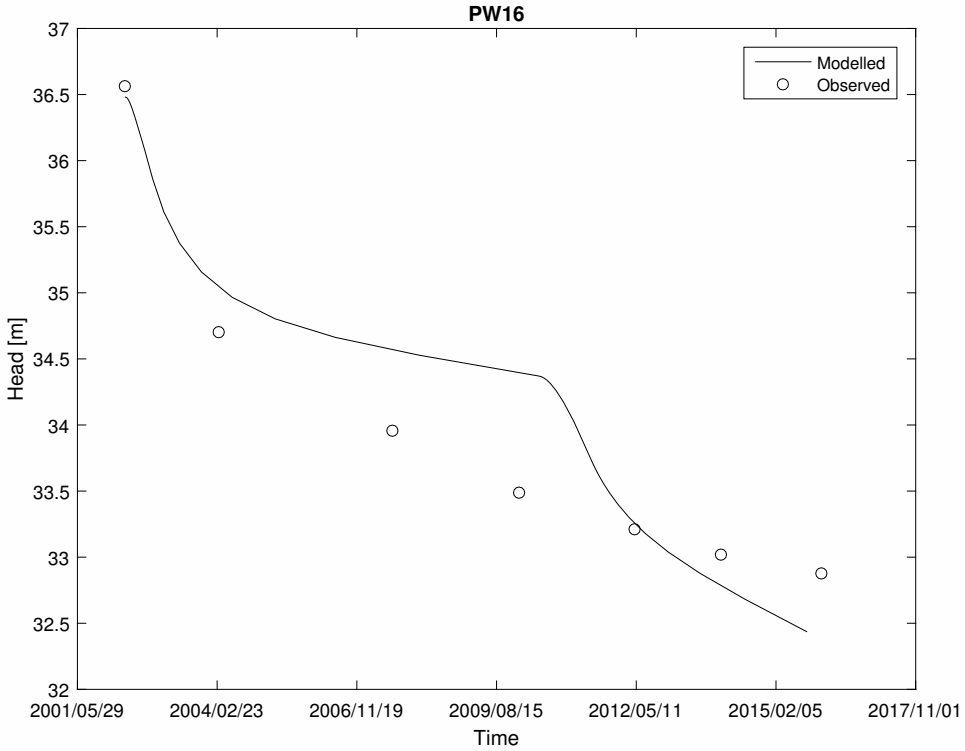

Figure 35: Modelled and observed head at pumping well 16.

5.1.7 Calibration Evaluation

The final parameter values in table 6 are accepted. Although the calibration targets were not met, the model is still believed to be sufficient for its purpose. More computing time and better calibration software could improve the calibration. The final parameter values provide a physically reasonable model as the head contours in April 2002, figures 36-38, and in December 2016, figures 39-41, show.

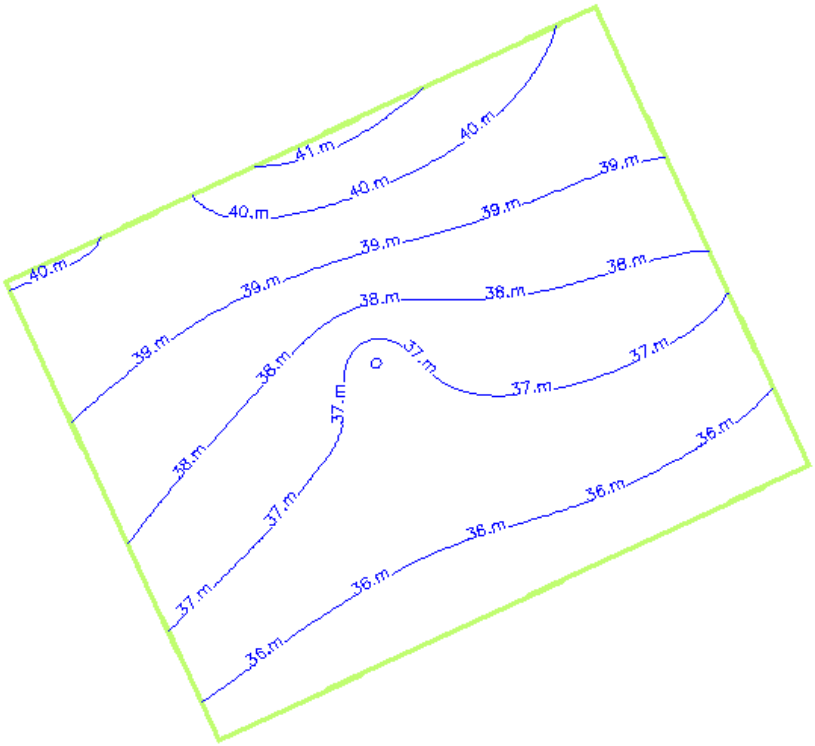

Figure 36: Spatial head distribution in layer 1 in April 2002.

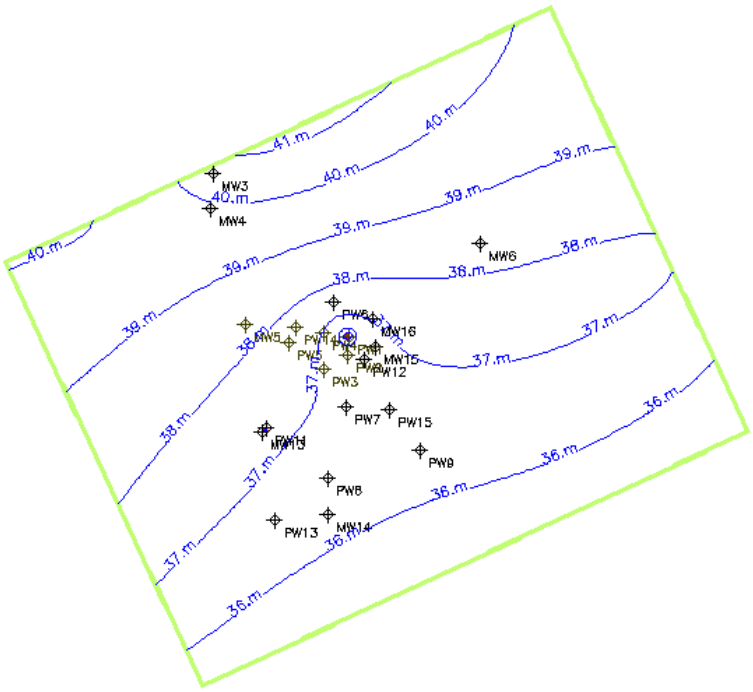

Figure 37: Spatial head distribution in layer 2 in April 2002.

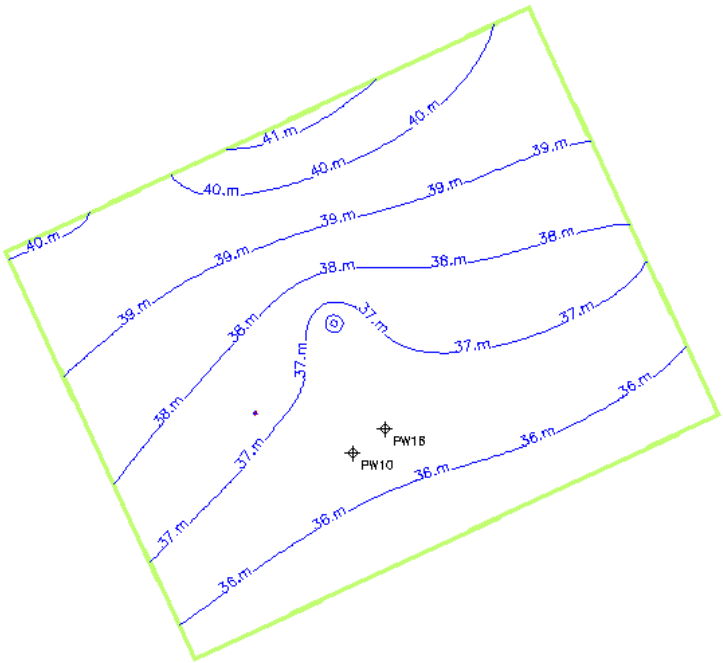

Figure 38: Spatial head distribution in layer 3 in April 2002.

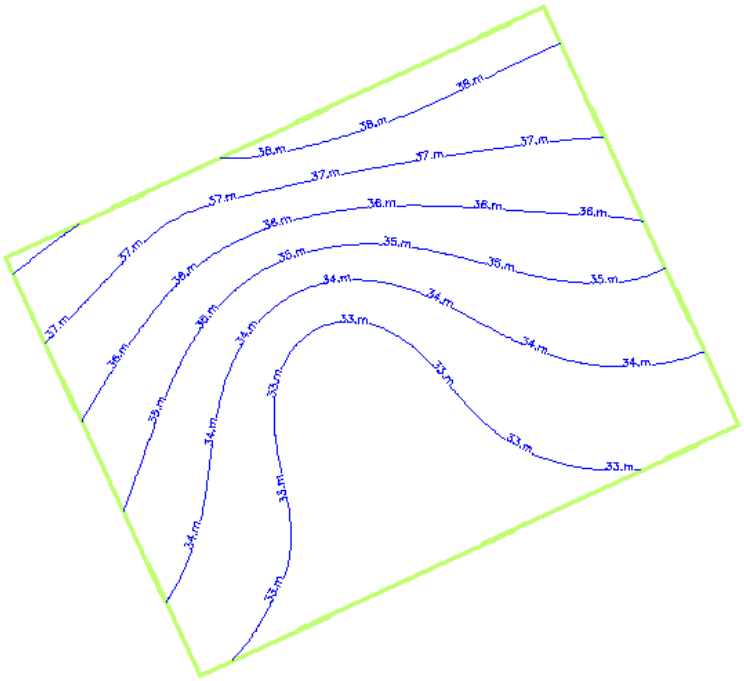

Figure 39: Spatial head distribution in layer 1 in December 2016.

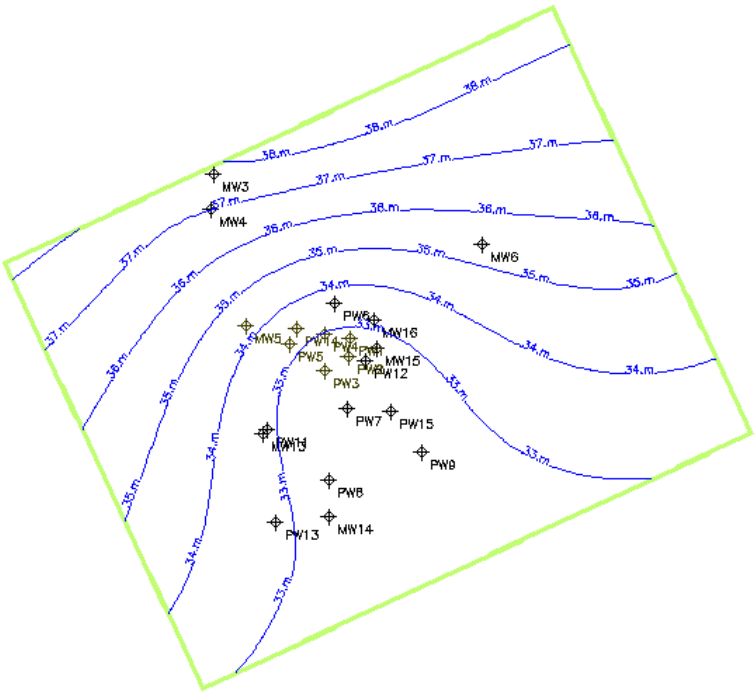

Figure 40: Spatial head distribution in layer 2 in December 2016.

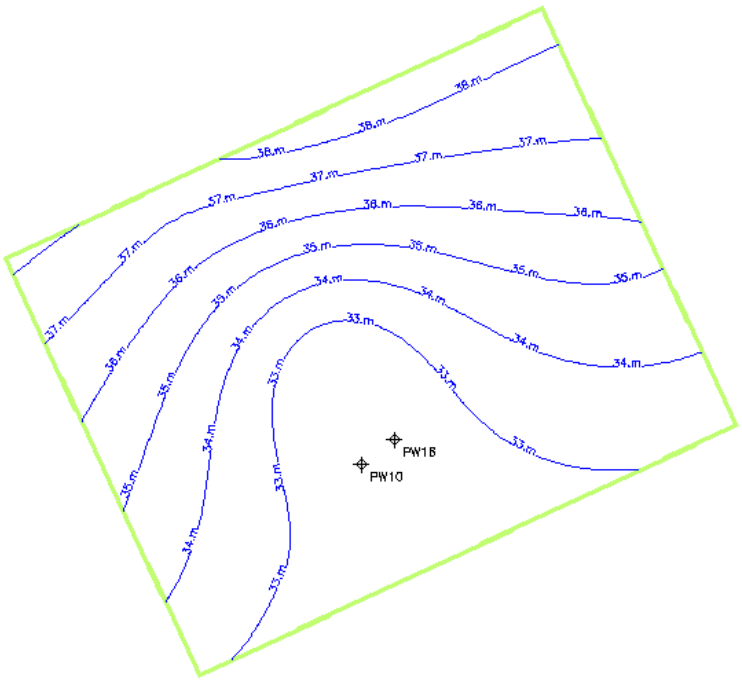

Figure 41: Spatial head distribution in layer 3 in December 2016.

5.2 Transport Model Calibration

5.2.1 Calibration Parameters

The transport model was calibrated for porosity, n, longitudinal horizontal dispersivity, α_L, transverse horizontal dispersivity, α_{TH} and transverse vertical dispersivity, α_{TV}.

5.2.2 Calibration and Verification Data

Calibration data consists of concentration observations from pumping wells 1-5, 14 and monitoring well 5 and can be seen in appendix (section 9.2.2). No part of the data is considered verification data as the calibration was done manually.

5.2.3 Calibration Targets

To evaluate the calibration, three calibration targets are defined:

$$\Delta t_{start,i} = |t_{start,i} - t^*_{start,i}| \tag{12}$$

where $t_{start,i}$ is the time of the first non-zero observed concentration at well i and t^*_{start} is the first modelled concentration at well i greater than $5 \cdot 10^{-8}\text{kg/m}^3$ (a value chosen arbitrarily to avoid numerical errors),

$$\Delta t_{peak,i} = |t_{peak,i} - t^*_{peak,i}| \tag{13}$$

where $t_{peak,i}$ is time of the peak observed concentration at well i and $t^*_{peak,i}$ is the time of the peak modelled concentration at well i and

$$\Delta C_{peak,i} = \frac{|C_{peak,i} - C^*_{peak,i}|}{C_{peak,i}} \cdot 100\% \tag{14}$$

where $C_{peak,i} = \max(C_i)$ is the peak observed concentration at well i over all time steps and $C^*_{peak,i} = \max(C^*_i)$ is the peak modelled concentration at well i. As a peak concentration can only be observed for pumping wells 4, 5 and 14 only they have a value for Δt_{peak} and ΔC_{peak}. Monitoring well 5 (MW5) is omitted from calibration evaluation as the model calculates a concentration of zero at this location throughout the simulation. Calibration targets are set as follows:

1. $\Delta t_{start} < 100\text{d}$ at any 3 wells,
2. $\Delta t_{peak} < 100\text{d}$ at any 2 wells,
3. and $\Delta C_{peak} < 50\%$ at any 3 wells.

5.2.4 Calibration Procedure

The calibration for the transport model is done manually, as opposed to how calibration of the flow model is handled. The initial values, i.e. values for the first iteration of calibration, are based on what can be thought of as reasonable parameter values for any aquifer and then updated manually until calibrations targets are met or considered sufficiently close. The parameter values are updated based on how the modelled breakthrough curves match the observed breakthrough curves.

5.2.5 Final Parameter Values

The final parameter values are found in table 7.

Table 7: Values for numerical transport model parameters.

Parameter	Value
n	0.12
α_L	5m
α_{TH}	1m
α_{TV}	0.25m

5.2.6 Calibration Results

Figures 42, 43, 44, 45, 46, 47 and 48 modelled and observed breakthrough curves for each well where MTBE has been observed.

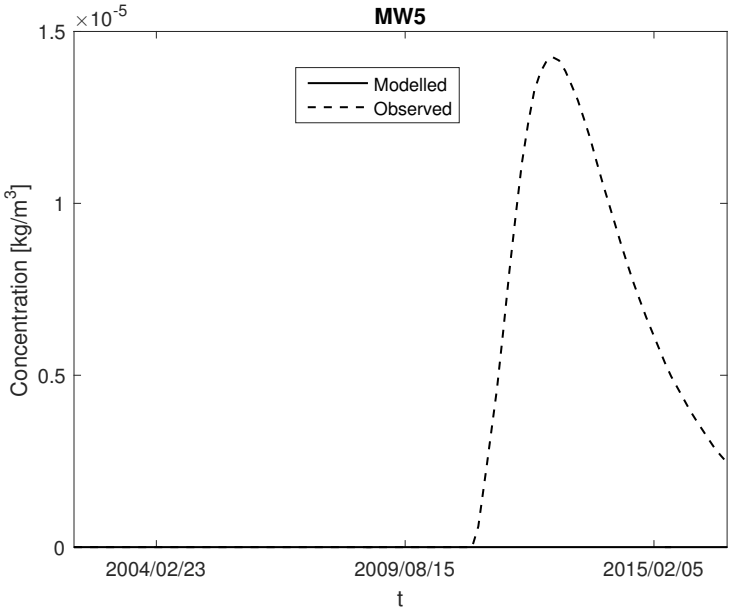

Figure 42: Modelled and observed concentration of MTBE as a function of time at monitoring well 5.

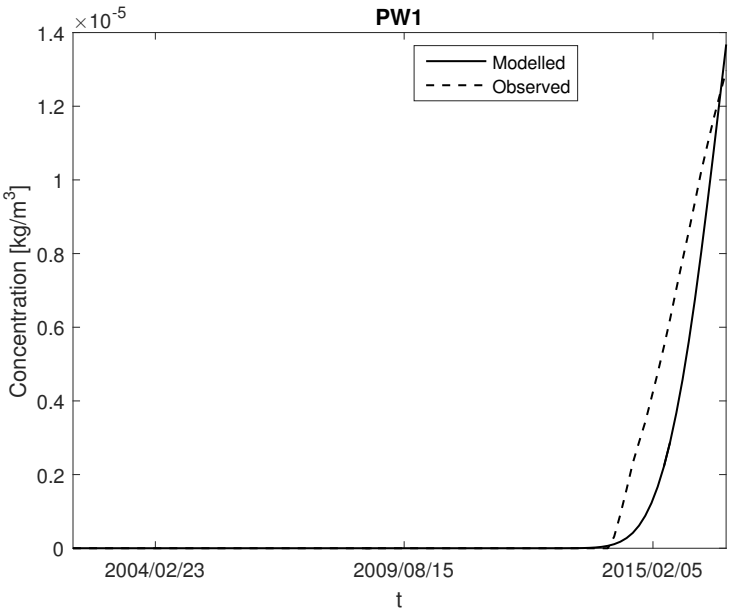

Figure 43: Modelled and observed concentration of MTBE as a function of time at pumping well 1.

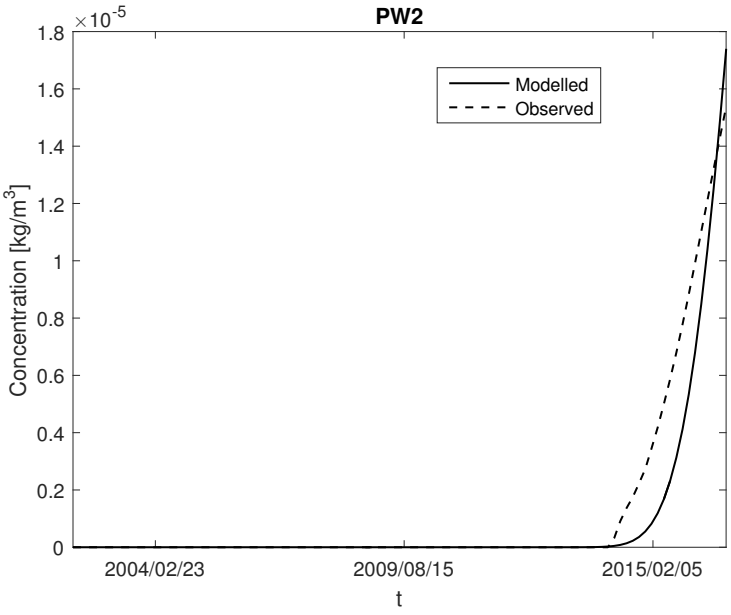

Figure 44: Modelled and observed concentration of MTBE as a function of time at pumping well 2.

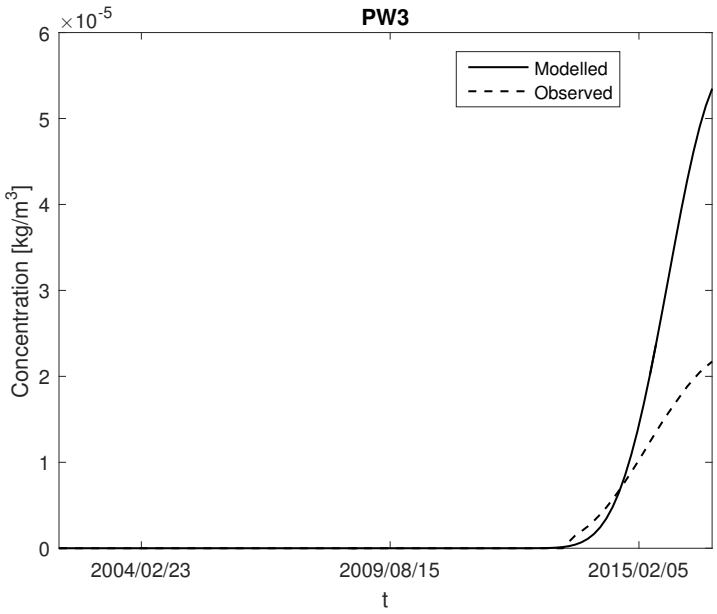

Figure 45: Modelled and observed concentration of MTBE as a function of time at pumping well 3.

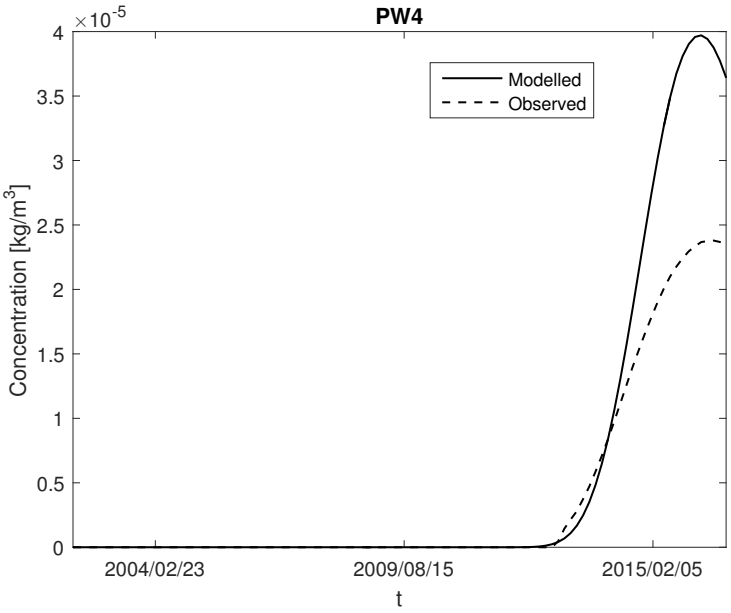

Figure 46: Modelled and observed concentration of MTBE as a function of time at pumping well 4.

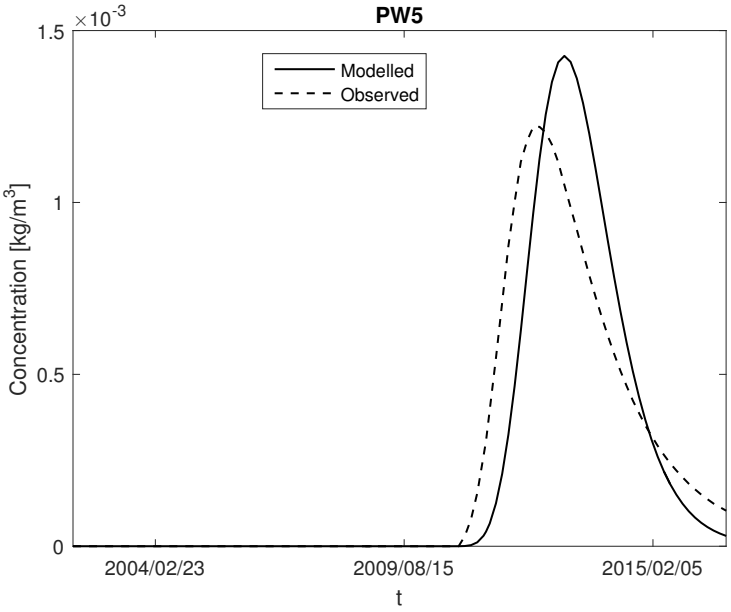

Figure 47: Modelled and observed concentration of MTBE as a function of time at pumping well 5.

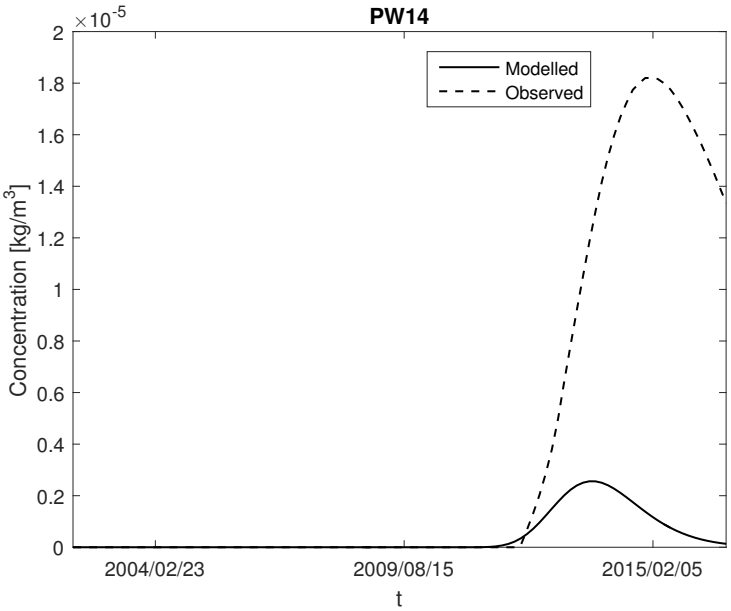

Figure 48: Modelled and observed concentration of MTBE as a function of time at pumping well 14.

To calculate the calibration evaluation measures, $t_{start}, t^*_{start}, t_{peak}, t^*_{peak}, C_{peak}$ and C^*_{peak} are determined and shown in table 8.

Table 8: Results of transport model calibration used for evaluating calibration targets.

	PW1	PW2	PW3	PW4	PW5	PW14
t_{start}	2014-02-07	2014-05-18	2013-04-13	2012-08-06	2010-10-26	2011-10-11
t^*_{start}	2014-03-29	2014-03-29	2013-07-22	2013-01-03	2010-12-15	2012-03-25
t_{peak}	-	-	-	2016-02-27	2013-02-22	2013-09-10
t^*_{peak}	-	-	-	2016-06-06	2012-06-17	2014-12-04
C_{peak}	-	-	-	$4.0 \cdot 10^{-5}$kg/m^3	$1.4 \cdot 10^{-3}$ kg/m^3	$2.6 \cdot 10^{-6}$kg/m^3
C^*_{peak}	-	-	-	$2.4 \cdot 10^{-5}$kg/m^3	$1.2 \cdot 10^{-3}$kg/m^3	$1.8 \cdot 10^{-5}$kg/m^3

Calibration evaluations are found in table 9.

Table 9: Results of transport model calibration evaluation.

Evaluation Parameter	PW1	PW2	PW3	PW4	PW5	PW14
Δt_{start}	50d	50d	100d	150d	50d	150d
Δt_{peak}	-	-	-	100d	250d	450d
ΔC_{peak}	-	-	-	67%	17%	86%

5.2.7 Calibration Evaluation

As seen in table 9, calibration target 3 is not met. The transport model could be improved with regards to matching peak concentrations but will suffice for the purpose of the model. Uncertainties of the transport model will be considered when discussing results.

6 Proposed Pumping Scheme

6.1 Requirements

The requirements for the new pumping scheme are:

1. Concentration in all water extracted from the pumping wells after June 2017 is less than the primary drinking water standard for MTBE ($1.3 \cdot 10^{-5}$kg/m^3).
2. The total pumping rate in all wells is 11,845 m^3/d at all times.
3. The pumping rate in all wells is sustainable at all times.

6.2 Background Study

To provide a pumping scheme that would meet the requirements stated in the previous section, the flow and transport model was simulated using current pumping conditions: well 1 & 11 have been pumping prior to 2002, while wells 1-8 and 11 have been pumping since May 1, 2002, remaining wells have been installed but are not pumping. Results of this simulation were analyzed to determine which wells detected concentrations above the primary drinking standard, see table 10. Dates are presented as month and year to reflect the uncertainty in the model.

Table 10: Results of background study. Start of Contamination is defined as first date of exceeding the primary drinking standard. End of Contamination is defined as the last date of exceeding the primary drinking standard. End of Contamination marked with "x" indicates that MTBE concentration is above the primary drinking water standard at end of simulation (December 31, 2032). Any pumping well not shown does not observe a concentration above the primary drinking standard at any time step.

Pumping Well	Start of Contamination	End of Contamination
1	September 2016	August 2017
2	July 2016	August 2028
3	January 2015	x
4	May 2018	January 2018
5	May 2011	April 2017
7	September 2025	x

6.3 Proposed Pumping Scheme

Requirement 1 sets a limit for concentration at all pumping wells after June 1, 2017, which corresponds to stress periods 3 and 4 in the model. Requirement 2 and 3 are satisfied for stress periods 0, 1 and 2 but need to be evaluated for the proposed pumping scheme, see section 7. The proposed pumping scheme describes which wells should be activated from stress period 3, starting in June 2011, and if they should be deactivated for stress period 4, starting in June 2017. At times earlier than June 2011, the pumping follows what has been previously stated, wells 1 and 11 have been pumping since May 2002.

The background study which resulted in table 10 provided information for an initial pumping scheme, which was altered in an iterative process to satisfy all requirements. The final pumping scheme, which is the pumping scheme this document thus proposes, is seen in table 11.

Table 11: Proposed pumping scheme. Pumping rates are set for every stress period due to the temporal discretization. Pumping wells not shown in a stress period are deactivated in that stress period.

Pumping Well	Pumping Rate [m^3/d]
Stress Period 3	
1-5	0
6	1180
7-9	1185
10	0
11-13	1185
14	0
15-17	1185
Stress Period 4	
1-5	0
6	4400
7-8	0
9	1481
10	0
11	500
12	0
13	4900
14-15	0
16	564
17	0

7 Simulation Results

All results shown in this section are simulated using the pumping scheme proposed in this report and the model presented in the numerical formulation. Pumping wells where simulated MTBE concentrations are above the primary drinking standard are shown in table 12.

Table 12: Results of simulation using proposed pumping scheme. Start of Contamination is defined as first date of exceeding the primary drinking standard. End of Contamination is defined as the last date of exceeding the primary drinking standard. End of Contamination marked with "x" indicates that MTBE concentration is above the primary drinking water standard at end of simulation (December 31, 2032). Any pumping well not shown does not observe a concentration above the primary drinking standard at any time step.

Pumping Well	Start of Contamination	End of Contamination
3	January 2018	x
5	May 2011	November 2021
7	November 2029	x
8	August 2031	x
17	January 2028	x

7.1 Head Distributions

Figure 49 shows head distributions in December 2032. The modelled boundary conditions do not affect the simulated head distribution near any active pumping well.

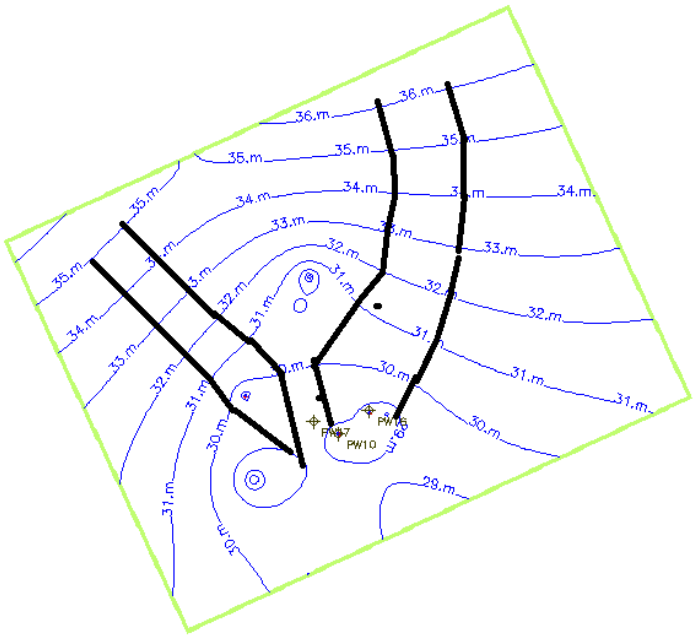

Figure 49: Head distribution at end of simulation (December 2032) in layer 3.

7.2 Breakthrough Curves

Figures 50-56 show breakthrough curves at all pumping wells where a concentration above the detection limit of MTBE ($1 \cdot 10^{-6}$kg/m^3) has been simulated. Observed concentrations, if provided, are shown as dark circles.

Pumping wells 3 and 4 have simulated concentrations of MTBE above the primary drinking standard in stress period 4 and is deactivated for stress periods 3 and 4. Pumping well 5 exceeds the standard in both stress periods which is why it is deactivated for both stress periods. Pumping wells 7 and 8 have simulated concentrations of MTBE above the standard in stress period 4 only, which is why they are deactivated for stress period 4. Pumping well 10 exceeds the standard by the end of stress period 4 and is deactivated in both stress periods 3 and 4. Pumping well 17 is active during stress period 3 but deactivated during stress period 4 where it exceeds the standard of MTBE.

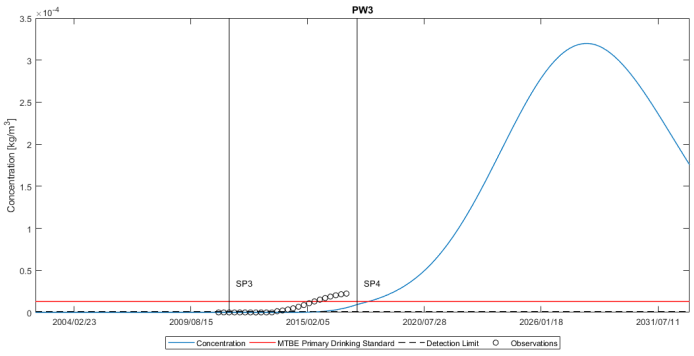

Figure 50: Breakthrough curve at pumping well 3. SP3 and SP4 indicate start of stress period 3 and 4 to the right of the vertical line.

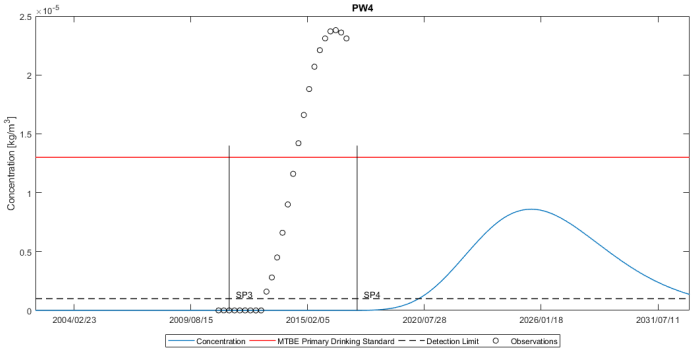

Figure 51: Breakthrough curve at pumping well 4. SP3 and SP4 indicate start of stress period 3 and 4 to the right of the vertical line.

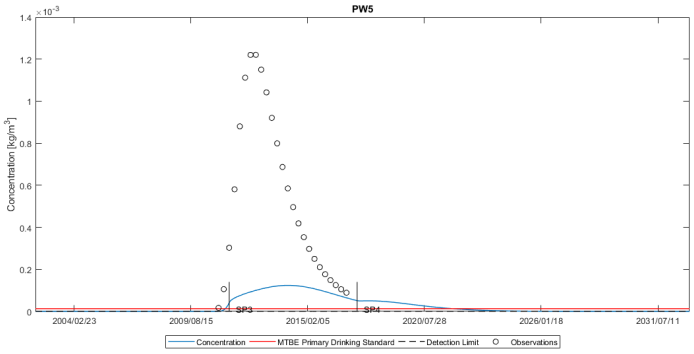

Figure 52: Breakthrough curve at pumping well 5. SP3 and SP4 indicate start of stress period 3 and 4 to the right of the vertical line.

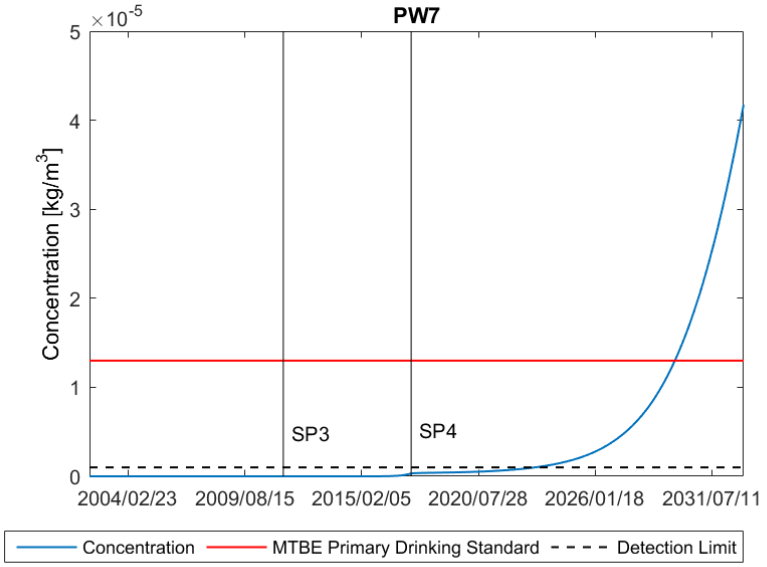

Figure 53: Breakthrough curve at pumping well 7. SP3 and SP4 indicate start of stress period 3 and 4 to the right of the vertical line.

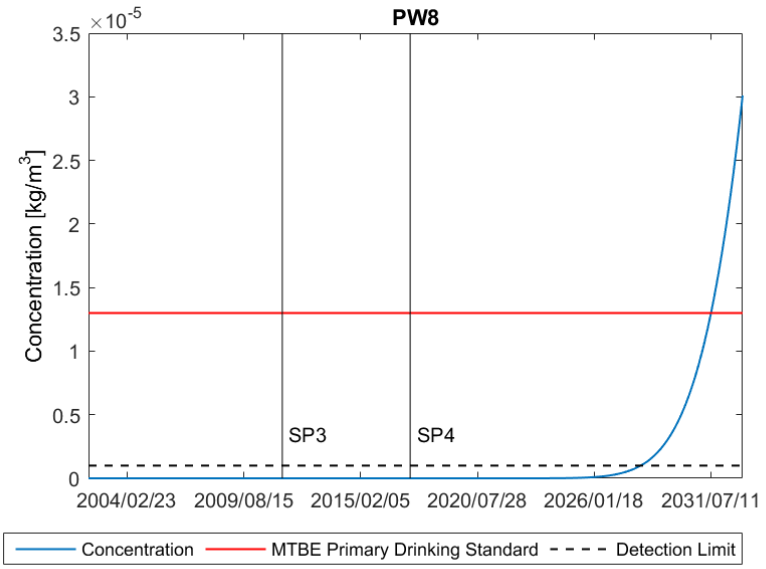

Figure 54: Breakthrough curve at pumping well 8. SP3 and SP4 indicate start of stress period 3 and 4 to the right of the vertical line.

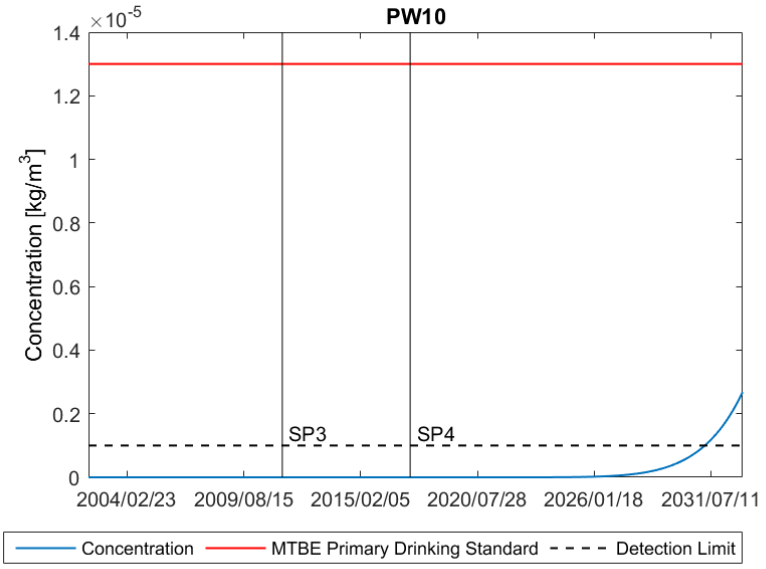

Figure 55: Breakthrough curve at pumping well 10. SP3 and SP4 indicate start of stress period 3 and 4 to the right of the vertical line.

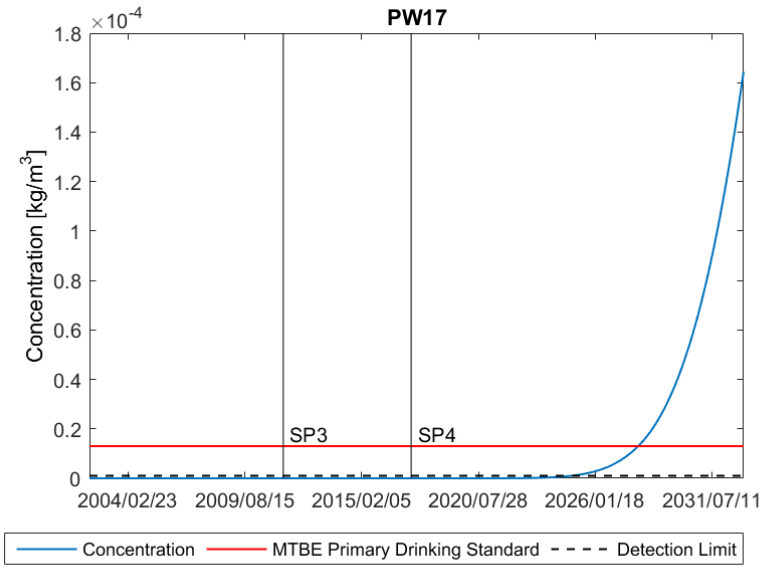

Figure 56: Breakthrough curve at pumping well 17. SP3 and SP4 indicate start of stress period 3 and 4 to the right of the vertical line.

7.3 Concentration Distributions

Figures 57-59 show concentration distributions in layer 1, 2 and 3 at end of simulation (December 2032).

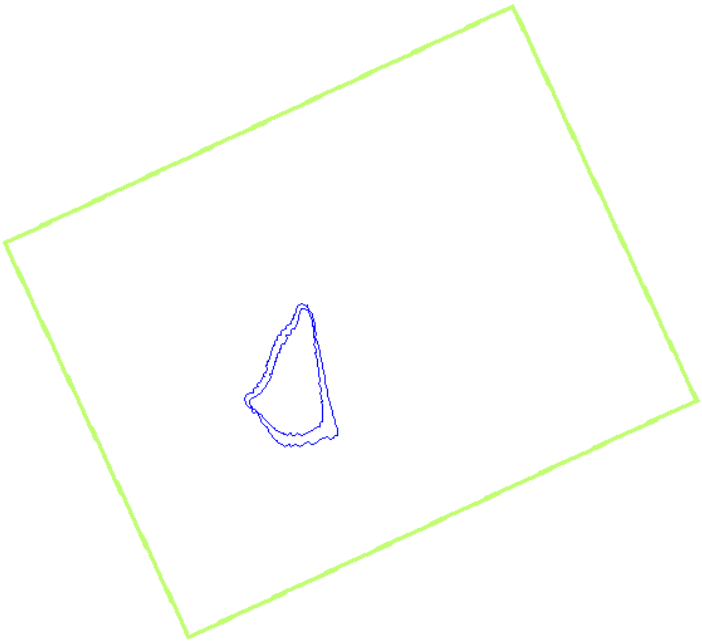

Figure 57: Concentration distribution in layer 1 in December 2032. Outer contour shows detection limit and inner contour shows primary drinking standard.

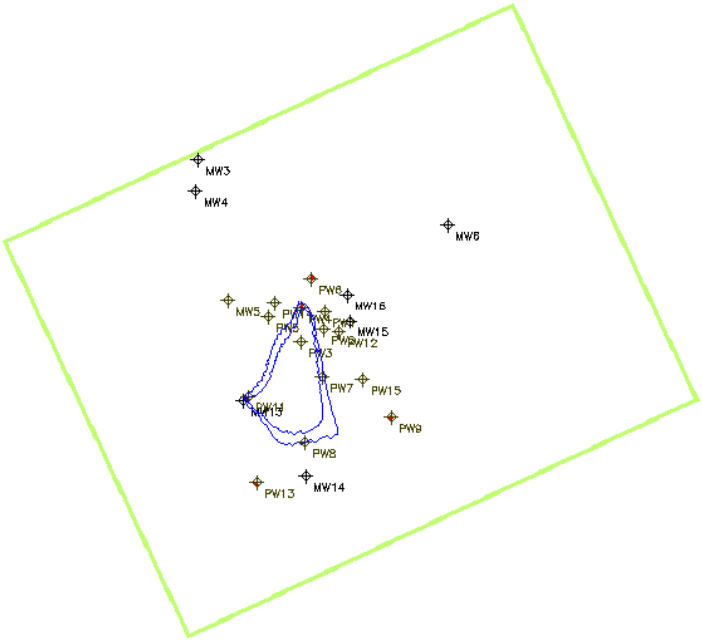

Figure 58: Concentration distribution in layer 2 in December 2032. Outer contour shows detection limit and inner contour shows primary drinking standard.

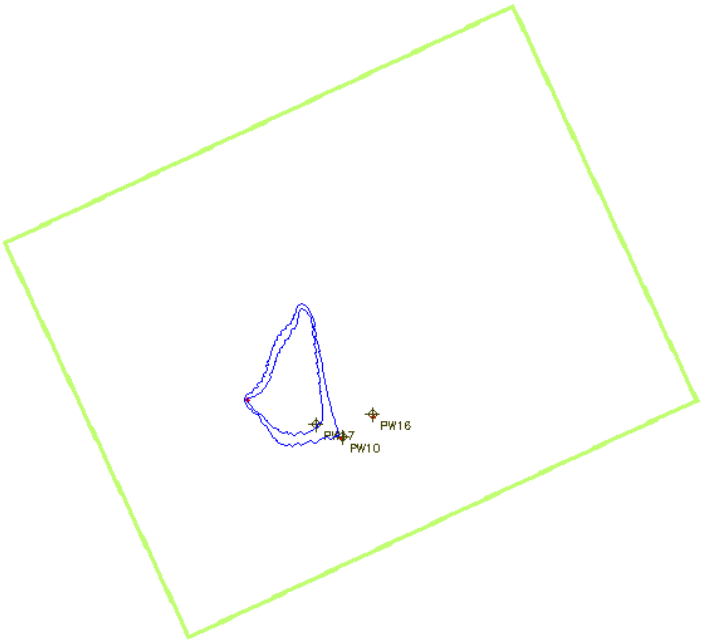

Figure 59: Concentration distribution in layer 3 in December 2032. Outer contour shows detection limit and inner contour shows primary drinking standard.

7.4 Future Modifications

Figures 60-76 show head at every pumping well as a function of time. No pumping well goes dry during the simulation in accordance with requirement 3. Pumping well 13 has head of 22m by the end of the simulation which should be accounted for when planning future operations.

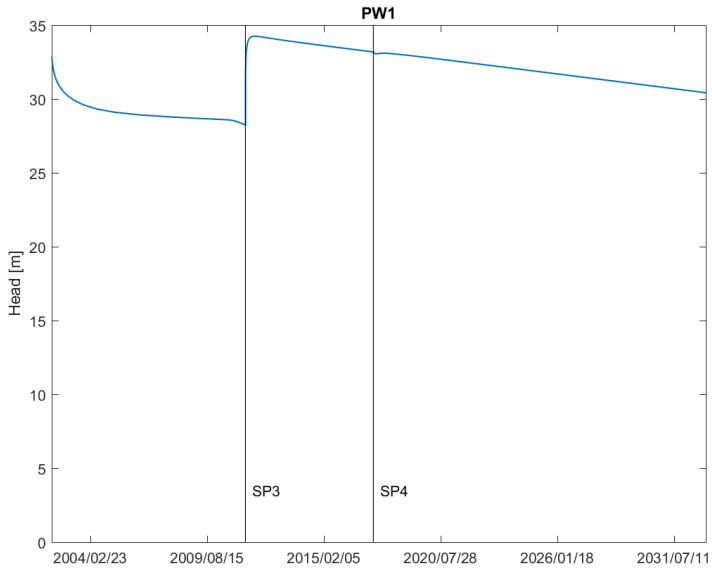

Figure 60: Head in pumping well 1 during simulation time. SP3 and SP4 vertical lines indicate start of respective stress period.

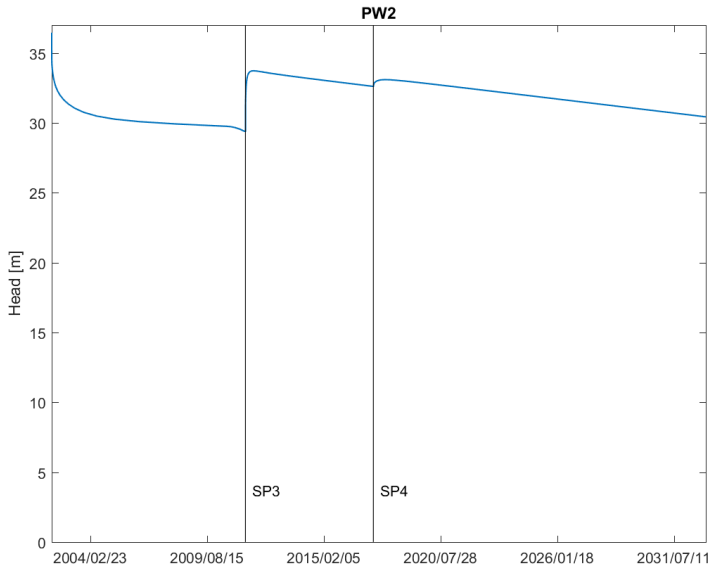

Figure 61: Head in pumping well 2 during simulation time. SP3 and SP4 vertical lines indicate start of respective stress period.

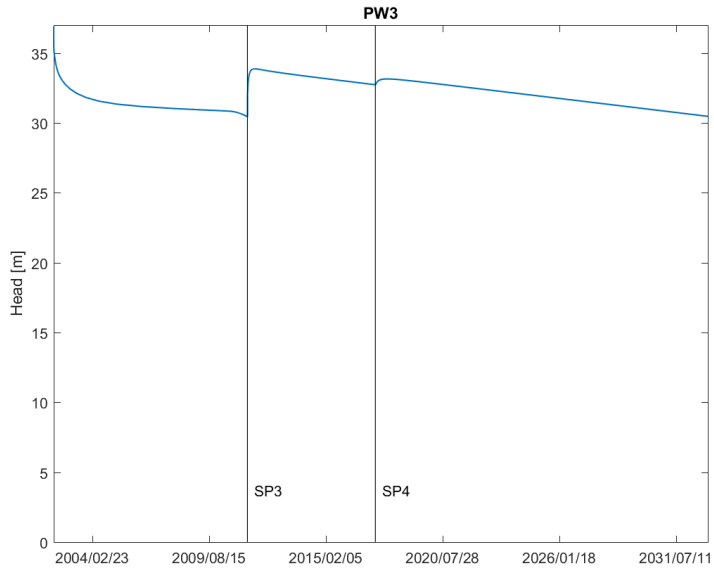

Figure 62: Head in pumping well 3 during simulation time. SP3 and SP4 vertical lines indicate start of respective stress period.

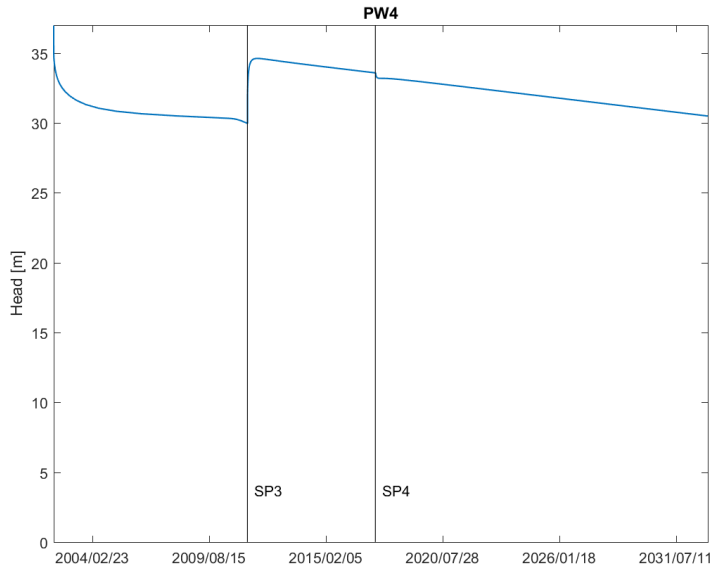

Figure 63: Head in pumping well 4 during simulation time. SP3 and SP4 vertical lines indicate start of respective stress period.

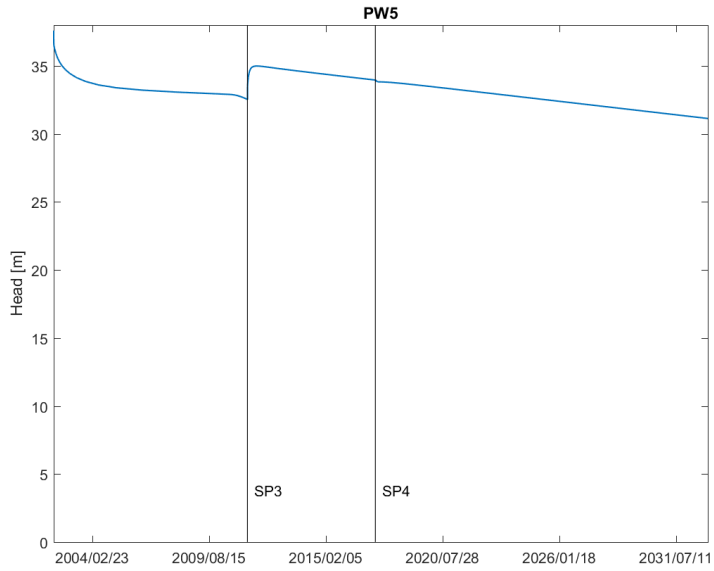

Figure 64: Head in pumping well 5 during simulation time. SP3 and SP4 vertical lines indicate start of respective stress period.

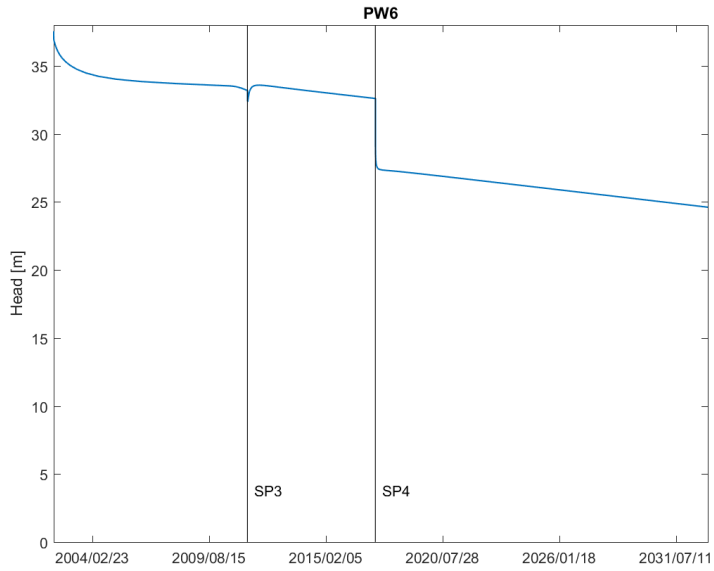

Figure 65: Head in pumping well 6 during simulation time. SP3 and SP4 vertical lines indicate start of respective stress period.

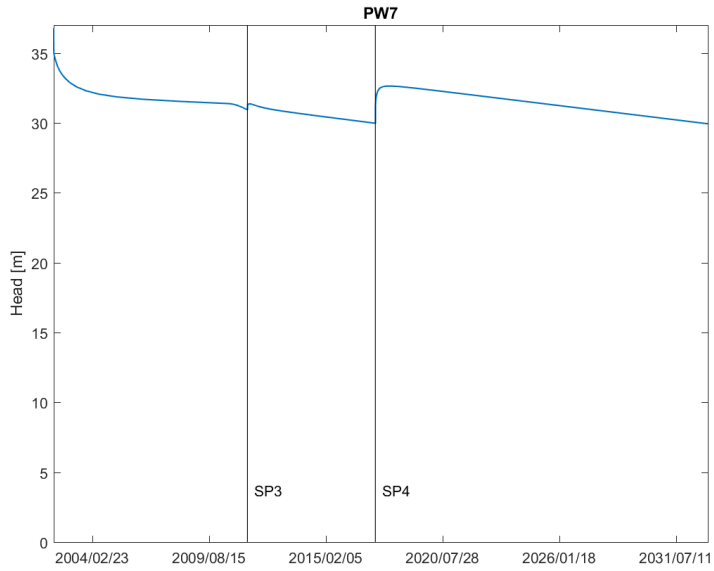

Figure 66: Head in pumping well 7 during simulation time. SP3 and SP4 vertical lines indicate start of respective stress period.

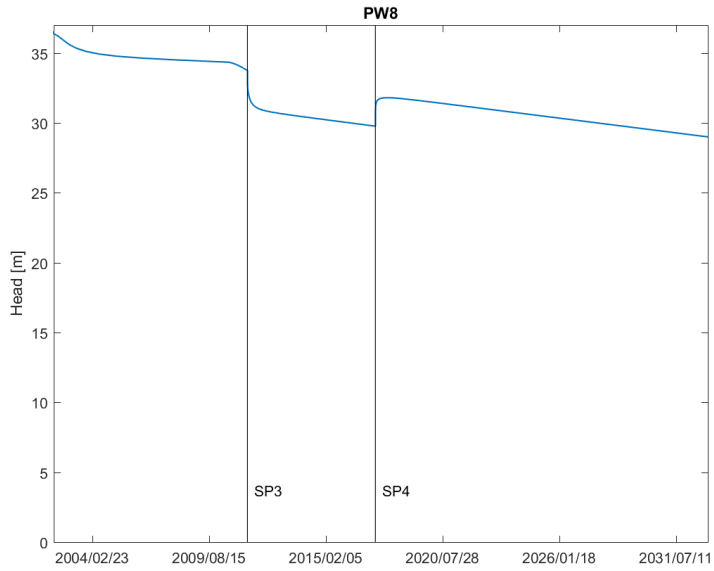

Figure 67: Head in pumping well 8 during simulation time. SP3 and SP4 vertical lines indicate start of respective stress period.

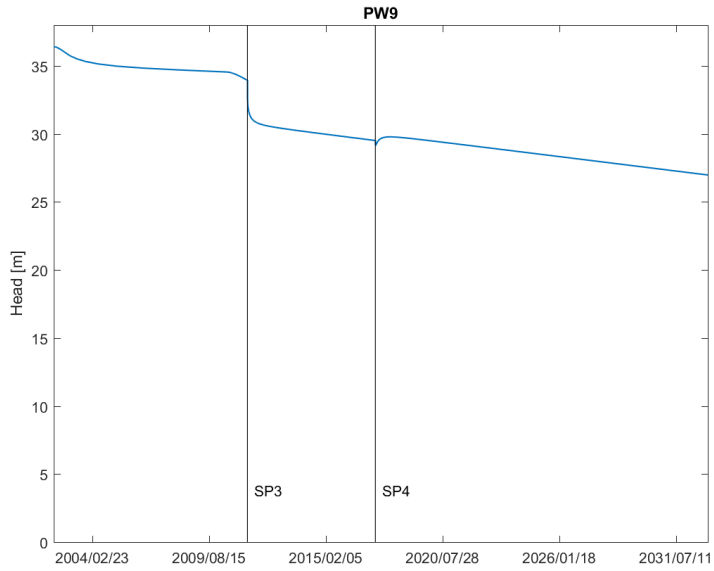

Figure 68: Head in pumping well 9 during simulation time. SP3 and SP4 vertical lines indicate start of respective stress period.

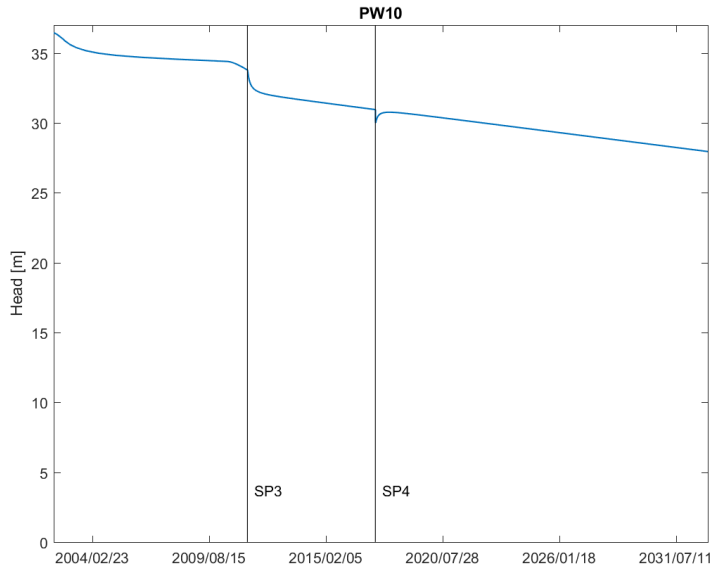

Figure 69: Head in pumping well 10 during simulation time. SP3 and SP4 vertical lines indicate start of respective stress period.

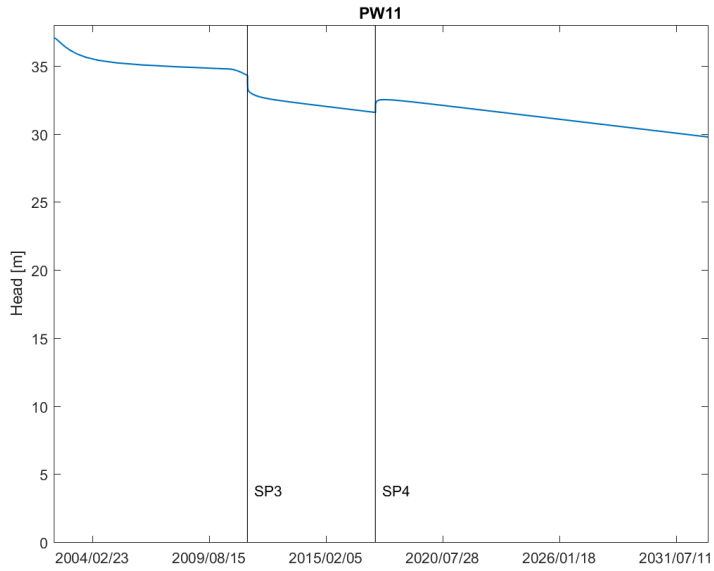

Figure 70: Head in pumping well 11 during simulation time. SP3 and SP4 vertical lines indicate start of respective stress period.

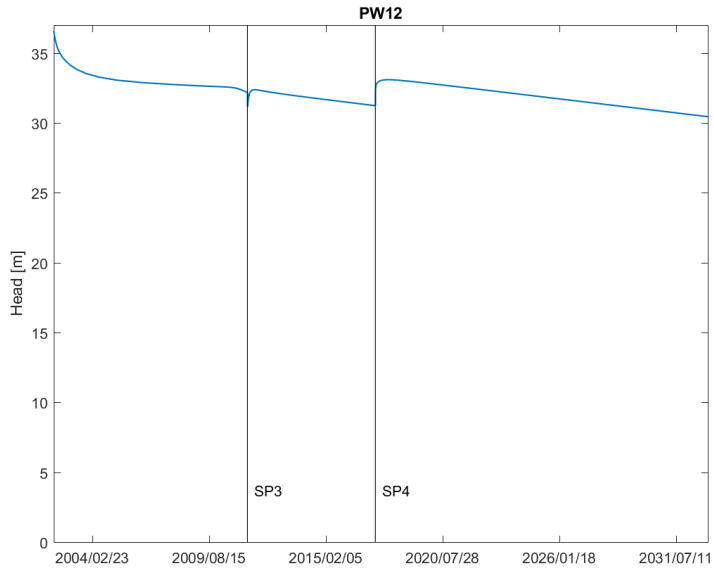

Figure 71: Head in pumping well 12 during simulation time. SP3 and SP4 vertical lines indicate start of respective stress period.

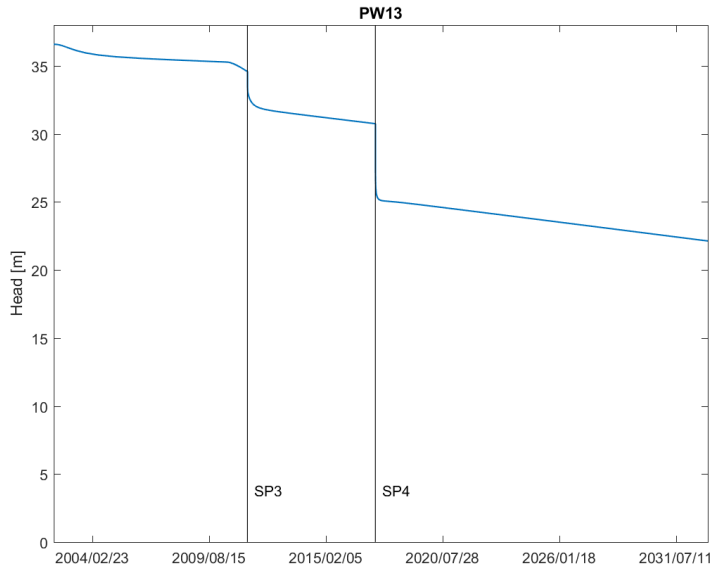

Figure 72: Head in pumping well 13 during simulation time. SP3 and SP4 vertical lines indicate start of respective stress period.

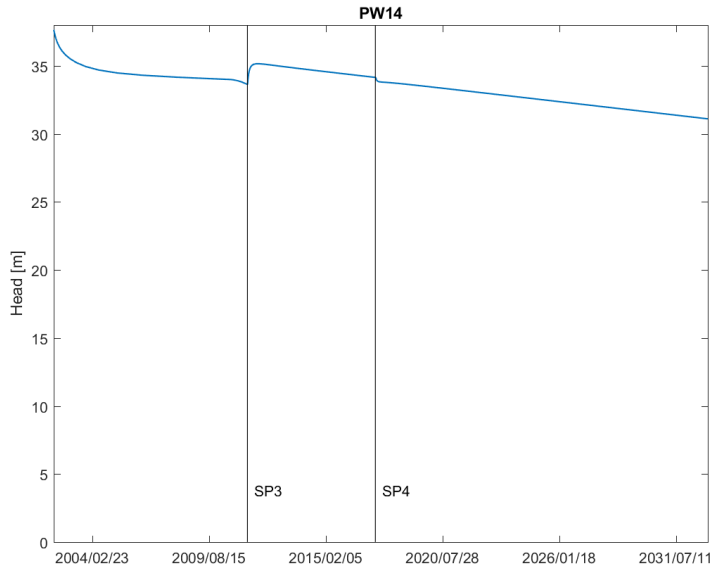

Figure 73: Head in pumping well 14 during simulation time. SP3 and SP4 vertical lines indicate start of respective stress period.

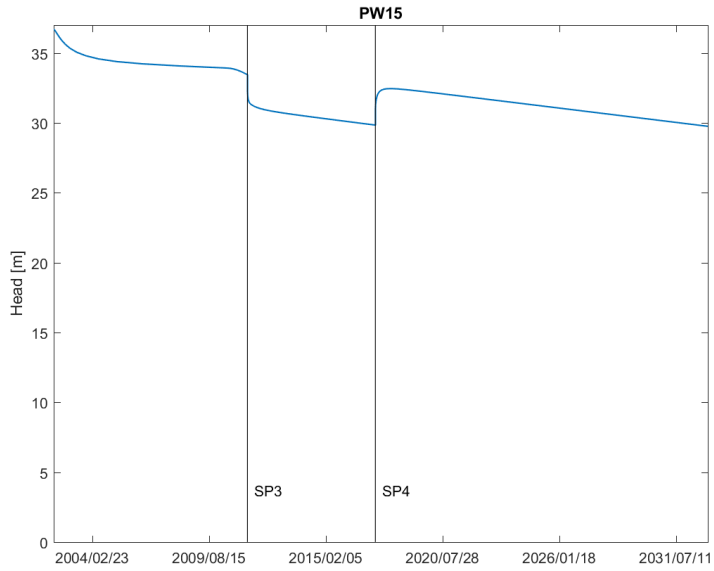

Figure 74: Head in pumping well 15 during simulation time. SP3 and SP4 vertical lines indicate start of respective stress period.

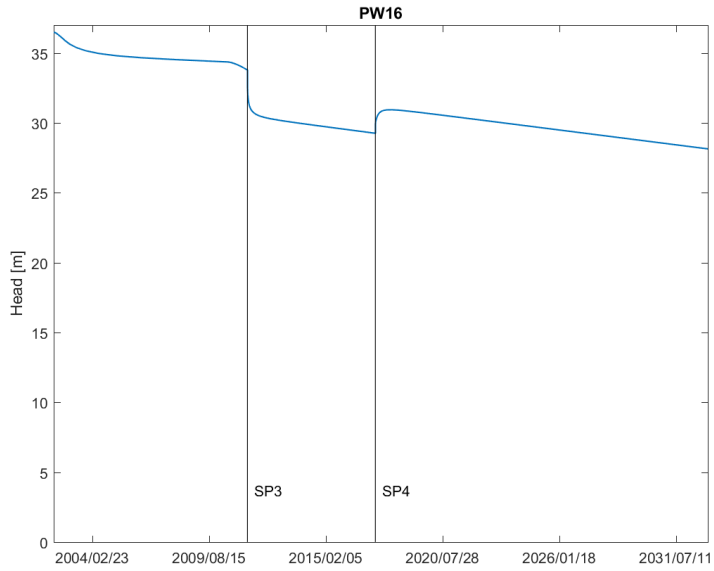

Figure 75: Head in pumping well 16 during simulation time. SP3 and SP4 vertical lines indicate start of respective stress period.

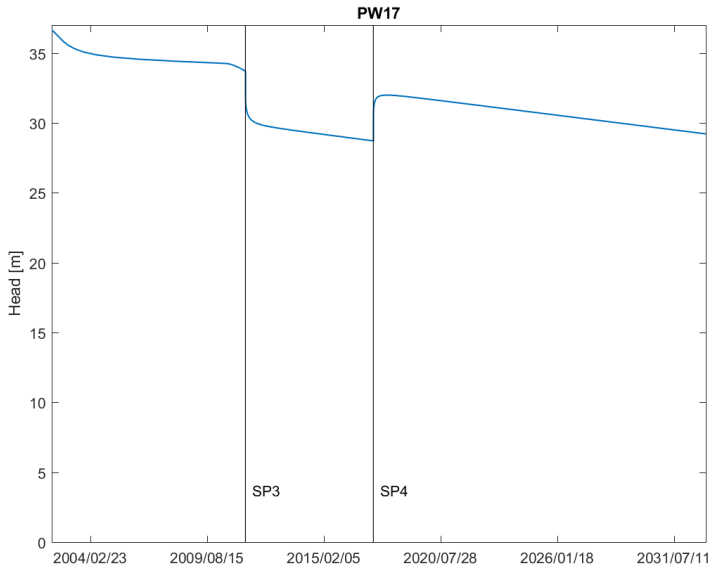

Figure 76: Head in pumping well 17 during simulation time. SP3 and SP4 vertical lines indicate start of respective stress period.

8 References

Anderson, Mary P., William W. Woessner, and R. J. Hunt (2015). *Applied Groundwater Modeling: Simulation of Flow and Advective Transport*. Second edition. OCLC: ocn921253555. London ; San Diego, CA: Academic Press. 564 pp. ISBN: 978-0-12-058103-0.

Bedekar, Vivek, Eric D. Morway, Christian D. Langevin, and Matthew J. Tonkin (2016). *MT3D-USGS Version 1: A US Geological Survey Release of MT3DMS Updated with New and Expanded Transport Capabilities for Use with MODFLOW*. US Geological Survey. URL: https://pubs.er.usgs.gov/publication/tm6A53 (visited on 05/03/2017).

Chiang, Wen-Hsing and Wolfgang Kinzelbach (2003). *3D-Groundwater Modeling with PMWIN: A Simulation System for Modeling Groundwater Flow and Pollution*. 3rd corrected printing. Berlin ; New York: Springer. 346 pp. ISBN: 978-3-540-67744-4.

Fitts, Charles R. (2013). *Groundwater Science*. Second edition. Amsterdam: Academic Press. 672 pp. ISBN: 978-0-12-384705-8.

Gelhar, Lynn W., Claire Welty, and Kenneth R. Rehfeldt (1992). "A Critical Review of Data on Field-Scale Dispersion in Aquifers". In: *Water Resources Research* 28.7, pp. 1955–1974. ISSN: 00431397. DOI: 10.1029/92WR00607. URL: http://doi.wiley.com/10.1029/92WR00607 (visited on 05/03/2017).

Harbaugh, Arlen W. (2005). *MODFLOW-2005, the US Geological Survey Modular Ground-Water Model: The Ground-Water Flow Process*. US Department of the Interior, US Geological Survey Reston, VA, USA. URL: http://md.water.usgs.gov/gw/modflow/MODFLOW_Docs/TM6-A16-MODFLOW-2005.pdf (visited on 05/03/2017).

Harbaugh, Arlen W., Christian D. Langevin, Joseph D. Hughes, and Richard G. Niswonger (2017). "MODFLOW: USGS Three-Dimensional Finite-Difference Groundwater Model". In: DOI: 10.5066/F7RF5S7G. URL: https://doi.org/10.5066/F7RF5S7G (visited on 05/03/2017).

Tonkin, Matthew J., Vivek Bedekar, Eric D. Morway, and Christian D. Langevin (2016). "MT3D-USGS: Groundwater Solute Transport Simulator for MODFLOW". In: DOI: 10.5066/F75T3HKD. URL: https://doi.org/10.5066/F75T3HKD (visited on 05/03/2017).

9 Appendices

9.1 Well Information

9.1.1 Pumping Wells

Table 13: Pumping wells information. Note that the pumping rate in this table is the pumping rate used by the city of Youngstown since May 2001.

Well Number	x (m)	y (m)	Land Surface Elevation (m)	Top of Well Screen (m)	Bottom of Well Screen (m)	Elevation of Bedrock (m)	Pumping Rate (m3/d)	Diameter (m)
1	5042	4881	39.96	9.15	4.91	-2.94	3120	0.5
2	5035	4597	38.96	8.77	4.37	-3.97	2120	0.5
3	4672	4384	36.83	3.79	-0.27	-10.43	1460	0.5
4	4664	4932	39.38	6.97	2.64	-7.28	1780	0.5
5	4145	4788	40.32	4.54	0.73	-8.74	980	0.5
6	4825	5399	38.68	6.66	2.27	-5.11	520	0.5
7	5008	3829	34.51	3.42	-1.10	-7.56	1470	0.5
8	4733	2774	34.46	2.24	-1.41	-8.57	180	0.5
9	6109	3175	38.10	7.73	3.90	-2.78	0	0.5
10	5321	2876	33.17	0.07	-4.02	-12.29	0	0.5
11	3814	3513	36.25	2.26	-1.25	-9.64	215	0.5
12	5280	4543	40.18	6.11	1.09	-7.13	0	0.5
13	3953	2136	37.32	6.24	2.42	-4.86	0	0.5
14	4249	5013	39.90	6.56	2.67	-8.05	0	0.5
15	5660	3790	36.64	3.07	-0.79	-8.47	0	0.5
16	5818	3241	35.51	-0.23	-5.65	-12.28	0	0.5
17	4943	3076	33.92	-1.47	-4.97	-13.49	0	0.5

9.1.2 Monitoring Wells

Table 14: Monitoring wells information.

Well Number	x (m)	y (m)	Land Surface Elevation (m)	Top of Well Screen (m)	Bottom of Well Screen (m)	Elevation of Bedrock (m)	Diameter (m)
1	1249	2603	37.54	5.69	1.16	-5.36	0.1
2	706	9573	44.86	8.20	3.00	-4.47	0.1
3	3022	7313	38.27	2.69	-0.18	-7.17	0.1
4	2984	6796	41.32	3.40	-0.72	-8.36	0.1
5	3503	5055	42.20	5.94	2.14	-7.98	0.1
6	7015	6267	39.03	7.08	2.74	-5.36	0.1
7	2870	8681	44.02	8.20	5.09	-0.61	0.1
8	6207	8406	37.07	4.51	0.04	-6.74	0.1
9	12708	5041	34.09	7.41	3.93	-3.09	0.1
10	12688	3085	33.28	-0.14	-2.77	-10.46	0.1
11	11937	1012	33.45	5.62	3.24	-4.65	0.1
12	7403	-435	32.96	5.96	2.16	-3.93	0.1
13	3746	3449	37.82	2.70	-0.66	-8.07	0.1
14	4741	2230	35.75	4.49	0.53	-7.16	0.1
15	5442	4721	40.91	8.35	3.80	-4.36	0.1
16	5402	5143	37.74	3.57	0.03	-7.51	0.1
17	6232	-1387	32.49	4.71	2.31	-5.46	0.1
18	4945	-1297	33.88	2.28	-0.61	-8.72	0.1

9.2 Calibration and Verification Data

9.2.1 Flow Model Calibration and Verification Data

Table 15: Head observations from pumping wells. All observations are expressed in meters.

Well	2001-04-30	2001-04-30	2007-01-08	2010-01-24	2012-04-25	2014-05-01	2015-12-22
1	33.64	29.23	28.25	27.64	27.29	27.04	26.87
2	36.41	30.08	29.11	28.51	28.18	27.94	27.78
3	36.99	31.55	30.63	30.07	29.75	29.53	29.37
4	36.98	31.31	30.38	29.81	29.49	29.26	29.10
5	37.76	33.61	32.76	32.23	31.93	31.72	31.57
6	37.70	34.23	33.38	32.86	32.56	32.34	32.20
7	36.85	32.15	31.29	30.75	30.45	30.23	30.08
8	36.64	34.61	33.91	33.45	33.18	32.98	32.85
9	36.50	34.85	34.14	33.67	33.40	33.21	33.08
10	36.50	34.65	33.94	33.48	33.21	33.02	32.88
11	37.15	35.09	34.36	33.89	33.62	33.42	33.29
12	36.62	32.82	31.93	31.38	31.06	30.84	30.69
13	36.63	35.43	34.81	34.39	34.14	33.96	33.83
14	37.77	34.39	33.54	33.02	32.72	32.51	32.36
15	36.76	34.33	33.54	33.03	32.74	32.54	32.40
16	36.56	34.70	33.96	33.49	33.21	33.02	32.88
17	36.70	34.51	33.77	33.30	33.02	32.82	32.68

Table 16: Head observations from monitoring wells. All observations are expressed in meters.

Well	2001-04-30	2004-02-03	2007-01-08	2010-01-24	2012-04-25	2014-05-01	2015-12-22
1	38.23	37.60	37.16	36.84	36.64	36.49	36.39
2	42.71	42.62	42.43	42.24	42.11	42.01	41.94
3	40.60	39.98	39.48	39.12	38.91	38.74	38.63
4	40.23	39.44	38.89	38.51	38.28	38.11	38.00
5	38.54	36.54	35.80	35.33	35.05	34.86	34.73
6	38.69	37.86	37.27	36.86	36.61	36.44	36.32
7	41.62	41.35	41.00	40.71	40.53	40.39	40.30
8	40.64	40.28	39.87	39.56	39.36	39.21	39.10
9	36.71	36.55	36.32	36.12	35.99	35.89	35.82
10	34.91	34.75	34.52	34.33	34.21	34.11	34.03
11	33.14	32.99	32.76	32.57	32.44	32.34	32.27
12	33.40	33.03	32.68	32.40	32.23	32.10	32.01
13	37.30	35.35	34.64	34.18	33.91	33.71	33.58
14	36.38	34.97	34.32	33.89	33.63	33.45	33.32
15	36.73	33.48	32.61	32.07	31.76	31.55	31.40
16	37.11	34.31	33.46	32.94	32.63	32.42	32.28
17	32.95	32.64	32.32	32.06	31.90	31.77	31.68
18	33.58	33.25	32.90	32.63	32.46	32.33	32.24

9.2.2 Transport Model Calibration Data

Table 17: Calibration data for transport model. All concentrations are in units of kg/m^3. Wells 1-5 and 14 are pumping wells 1-5 and 14. MW5 is monitoring well 5.

Date	Well 1	Well 2	Well 3	Well 4	Well 5	Well 14	MW5
2010-12-01	0.00E+00	0.00E+00	0.00E+00	0.00E+00	1.70E-05	0.00E+00	0.00E+00
2011-03-01	0.00E+00	0.00E+00	0.00E+00	0.00E+00	1.06E-04	0.00E+00	0.00E+00
2011-06-01	0.00E+00	0.00E+00	0.00E+00	0.00E+00	3.03E-04	0.00E+00	2.40E-06
2011-09-01	0.00E+00	0.00E+00	0.00E+00	0.00E+00	5.81E-04	0.00E+00	4.90E-06
2011-12-01	0.00E+00	0.00E+00	0.00E+00	0.00E+00	8.80E-04	0.00E+00	8.10E-06
2012-03-01	0.00E+00	0.00E+00	0.00E+00	0.00E+00	1.11E-03	0.00E+00	1.10E-05
2012-05-31	0.00E+00	0.00E+00	0.00E+00	0.00E+00	1.22E-03	1.10E-06	1.31E-05
2012-08-31	0.00E+00	0.00E+00	0.00E+00	0.00E+00	1.22E-03	2.40E-06	1.41E-05
2012-11-30	0.00E+00	0.00E+00	0.00E+00	0.00E+00	1.15E-03	4.30E-06	1.43E-05
2013-03-01	0.00E+00	0.00E+00	0.00E+00	1.60E-06	1.04E-03	6.70E-06	1.38E-05
2013-06-01	0.00E+00	0.00E+00	0.00E+00	2.80E-06	9.21E-04	9.20E-06	1.30E-05
2013-08-31	0.00E+00	0.00E+00	1.40E-06	4.50E-06	7.99E-04	1.16E-05	1.20E-05
2013-11-30	0.00E+00	0.00E+00	2.30E-06	6.60E-06	6.87E-04	1.38E-05	1.08E-05
2014-03-02	0.00E+00	0.00E+00	3.50E-06	9.00E-06	5.85E-04	1.56E-05	9.70E-06
2014-06-01	1.50E-06	1.10E-06	5.00E-06	1.16E-05	4.96E-04	1.69E-05	8.60E-06
2014-08-31	2.40E-06	1.80E-06	6.80E-06	1.42E-05	4.19E-04	1.78E-05	7.60E-06
2014-12-01	3.40E-06	2.70E-06	8.80E-06	1.66E-05	3.53E-04	1.82E-05	6.70E-06
2015-03-02	4.60E-06	4.00E-06	1.09E-05	1.88E-05	2.98E-04	1.82E-05	5.90E-06
2015-06-01	5.90E-06	5.50E-06	1.31E-05	2.07E-05	2.50E-04	1.79E-05	5.10E-06
2015-09-01	7.40E-06	7.20E-06	1.52E-05	2.21E-05	2.11E-04	1.73E-05	4.50E-06
2015-12-01	8.80E-06	9.10E-06	1.71E-05	2.31E-05	1.77E-04	1.65E-05	3.90E-06
2016-03-01	1.03E-05	1.11E-05	1.89E-05	2.37E-05	1.49E-04	1.56E-05	3.40E-06
2016-05-31	1.16E-05	1.31E-05	2.04E-05	2.38E-05	1.25E-04	1.46E-05	2.90E-06
2016-08-31	1.28E-05	1.51E-05	2.16E-05	2.36E-05	1.06E-04	1.35E-05	2.50E-06
2016-11-30	1.39E-05	1.70E-05	2.24E-05	2.31E-05	8.91E-05	1.25E-05	2.20E-06

9.2.3 Residuals from Flow Model Calibration

Table 18: Modelled heads, observed heads and residuals at each pumping well. All heads are expressed in units of meter.

Well		2001-04-30	2004-02-03	2007-01-08	2010-01-24	2012-04-25	2014-05-01	2015-12-22
PW1	**Observed**	33.64	29.23	28.25	27.64	27.29	27.04	26.87
	Modelled	32.88	29.43	28.82	28.61	27.63	27.05	26.62
	Residual	0.76	-0.20	-0.57	-0.97	-0.34	-0.01	0.25
PW2	**Observed**	36.41	30.08	29.11	28.51	28.18	27.94	27.78
	Modelled	36.46	30.60	29.98	29.77	28.77	28.19	27.76
	Residual	-0.05	-0.52	-0.87	-1.26	-0.59	-0.25	0.02
PW3	**Observed**	36.99	31.55	30.63	30.07	29.75	29.53	29.37
	Modelled	36.92	31.67	31.07	30.86	29.85	29.29	28.86
	Residual	0.07	-0.12	-0.44	-0.79	-0.10	0.24	0.51
PW4	**Observed**	36.98	31.31	30.38	29.81	29.49	29.26	29.10
	Modelled	36.97	31.16	30.55	30.35	29.37	28.80	28.37
	Residual	0.01	0.15	-0.17	-0.54	0.12	0.46	0.73
PW5	**Observed**	37.76	33.61	32.76	32.23	31.93	31.72	31.57
	Modelled	37.60	33.70	33.12	32.93	31.95	31.42	31.01
	Residual	0.16	-0.09	-0.36	-0.70	-0.02	0.30	0.56
PW6	**Observed**	37.70	34.23	33.38	32.86	32.56	32.34	32.20
	Modelled	37.56	34.33	33.75	33.55	32.63	32.08	31.67
	Residual	0.14	-0.10	-0.37	-0.69	-0.07	0.26	0.53
PW7	**Observed**	36.85	32.15	31.29	30.75	30.45	30.23	30.08
	Modelled	36.79	32.16	31.64	31.23	30.35	29.82	29.40
	Residual	0.06	-0.01	-0.35	-0.48	0.10	0.41	0.68
PW8	**Observed**	36.64	34.61	33.91	33.45	33.18	32.98	32.85
	Modelled	36.58	35.01	34.55	34.36	33.23	32.77	32.37
	Residual	0.06	-0.40	-0.64	-0.91	-0.05	0.21	0.48
PW9	**Observed**	36.50	34.85	34.14	33.67	33.40	33.21	33.08
	Modelled	36.41	35.22	34.76	34.57	33.43	32.97	32.56
	Residual	0.09	-0.37	-0.62	-0.90	-0.03	0.24	0.52
PW10	**Observed**	36.50	34.65	33.94	33.48	33.21	33.02	32.88
	Modelled	36.44	35.06	34.61	34.41	33.27	32.81	32.40
	Residual	0.06	-0.41	-0.67	-0.93	-0.06	0.21	0.48
PW11	**Observed**	37.15	35.09	34.36	33.89	33.62	33.42	33.29
	Modelled	37.05	35.50	34.98	34.79	33.74	33.25	32.85
	Residual	0.10	-0.41	-0.62	-0.90	-0.12	0.17	0.44
PW12	**Observed**	36.62	32.82	31.93	31.38	31.06	30.84	30.69
	Modelled	36.62	33.39	32.78	32.58	31.58	31.02	30.59
	Residual	0.00	-0.57	-0.85	-1.20	-0.52	-0.18	0.10
PW13	**Observed**	36.63	35.43	34.81	34.39	34.14	33.96	33.83
	Modelled	36.59	35.86	35.47	35.29	34.12	33.71	33.33
	Residual	0.04	-0.43	-0.66	-0.90	0.02	0.25	0.50
PW14	**Observed**	37.77	34.39	33.54	33.02	32.72	32.51	32.36
	Modelled	37.66	34.80	34.22	34.02	33.06	32.52	32.11
	Residual	0.11	-0.41	-0.68	-1.00	-0.34	-0.01	0.25
PW15	**Observed**	36.76	34.33	33.54	33.03	32.74	32.54	32.40
	Modelled	36.69	34.67	34.14	33.94	32.90	32.38	31.97
	Residual	0.07	-0.34	-0.60	-0.91	-0.16	0.16	0.43
PW16	**Observed**	36.56	34.70	33.96	33.49	33.21	33.02	32.88
	Modelled	36.48	35.05	34.57	34.38	33.27	32.79	32.38
	Residual	0.08	-0.35	-0.61	-0.89	-0.06	0.23	0.50

Table 19: Modelled heads, observed heads and residuals at each monitoring wells. All heads are expressed in units of meter.

Well		2001-04-30	2004-02-03	2007-01-08	2010-01-24	2012-04-25	2014-05-01	2015-12-22
MW3	**Observed**	40.60	39.98	39.48	39.12	38.91	38.74	38.63
	Modelled	40.50	40.34	40.11	39.94	38.59	38.26	37.90
	Residual	0.10	-0.36	-0.63	-0.82	0.32	0.48	0.73
MW4	**Observed**	40.23	39.44	38.89	38.51	38.28	38.11	38.00
	Modelled	39.91	39.53	39.23	39.06	37.93	37.56	37.21
	Residual	0.32	-0.09	-0.34	-0.55	0.35	0.55	0.79
MW5	**Observed**	38.54	36.54	35.80	35.33	35.05	34.86	34.73
	Modelled	38.30	36.69	36.16	35.97	35.02	34.53	34.14
	Residual	0.24	-0.15	-0.36	-0.64	0.03	0.33	0.59
MW6	**Observed**	38.69	37.86	37.27	36.86	36.61	36.44	36.32
	Modelled	38.38	37.82	37.35	37.18	36.39	35.91	35.55
	Residual	0.31	0.04	-0.08	-0.32	0.22	0.53	0.77
MW13	**Observed**	37.30	35.35	34.64	34.18	33.91	33.71	33.58
	Modelled	37.15	35.70	35.20	35.01	33.94	33.46	33.07
	Residual	0.15	-0.35	-0.56	-0.83	-0.03	0.25	0.51
MW14	**Observed**	36.38	34.97	34.32	33.89	33.63	33.45	33.32
	Modelled	36.32	35.41	35.01	34.83	33.64	33.22	32.83
	Residual	0.06	-0.44	-0.69	-0.94	-0.01	0.23	0.49
MW15	**Observed**	36.73	33.48	32.61	32.07	31.76	31.55	31.40
	Modelled	36.73	34.00	33.40	33.20	32.23	31.67	31.25
	Residual	0.00	-0.52	-0.79	-1.13	-0.47	-0.12	0.15
MW16	**Observed**	37.11	34.31	33.46	32.94	32.63	32.42	32.28
	Modelled	37.07	34.68	34.09	33.89	32.97	32.41	32.00
	Residual	0.04	-0.37	-0.63	-0.95	-0.34	0.01	0.28